INTERACTION

OF

WAVES AND A SHEAR FLOW

by

BLYTH ALVIN HUGHES
B.A., University of British Columbia, 1956

A THESIS SUBMITTED IN PARTIAL FULFILMENT OF
THE REQUIREMENTS FOR THE DEGREE OF
MASTER OF ARTS
in the Department
of
PHYSICS

We accept this thesis as conforming to the required standard:

THE UNIVERSITY OF BRITISH COLUMBIA

June, 1960

In presenting this thesis in partial fulfilment of the requirements for an advanced degree at the University of British Columbia, I agree that the Library shall make it freely available for reference and study. I further agree that permission for extensive copying of this thesis for scholarly purposes may be granted by the Head of my Department or by his representatives. It is understood that copying or publication of this thesis for financial gain shall not be allowed without my written permission.

Department of Physics

The University of British Columbia,
Vancouver 8, Canada.

Date June 20, 1960

ABSTRACT

A series of experiments has been undertaken in which three major properties of a surface tension-gravity wave system have been critically examined. The results of these experiments have been compared with existing theories. The three properties are: viscous decay in the absence of mean flow, which has been compared to the theory given in Lamb (1932) #348; propagation velocities in the presence and absence of mean flow, compared to Lamb (1932) #267, and the change of wave energy on crossing a stable Couette shear flow, compared to two theories - one obtained from the Navier-Stokes equations including terms up to second order in wave slope; the other, following previous authors, assuming any direct interaction of the waves with the shear flow to be negligible. According to the theory obtained from the Navier-Stokes equations the divergence of the rate of transport of surface wave energy is equal to the rate of change of wave energy due to the interaction of the mean flow and the wave system plus the rate of change of energy due to viscous decay.

An optical system was used to measure the maximum wave slope, the wavenumbers and the shear velocities. A grid of point source lights was set up to reflect off a previously chosen part of the shear flow into a properly oriented camera. A series of pulses of waves, generated by an electromechanical transducer, were then sent across this region of the flow.

For each pulse of waves a photograph was taken of the oscillating images of the lights with the exposure time longer than one wave period. The resulting streaks on the film are proportional to the maximum wave slopes at the positions from which the undeviated light reflects. A series of parallel straight white strings were photographed with the aid of a flash unit when waves crossed the flow. This was then used to determine lines of constant phase from which the wavelength and hence the wavenumber was measured at various positions across the flow. The viscous decay and part of the propagation measurements were obtained in this way but with no mean flow.

Results indicate that an anomalous region of wave properties exists for wavenumbers near 2.7 $cm.^{-1}$. For a set of data in which the wavenumbers were always less than 1.8 $cm.^{-1}$, it was found that the viscous decay rate and the propagation laws agree with theory to within the experimental error, and the interaction measurements fit the theory with the non-linear term included rather than the traditional theories.

TABLE OF CONTENTS

TABLE OF CONTENTS (continued)

LIST OF ILLUSTRATIONS

ACKNOWLEDGMENT

I should like to thank Dr. R.W. Stewart for his expert supervision and for the many ideas that were contributed by him. I should also like to thank Mr. J.C. Archer for his technical assistance.

INTRODUCTION

The work discussed herein is a critical experimental investigation of three major properties of surface waves in the regime where both surface tension and gravity are important. These properties are: viscous dissipation in the absence of any mean flow, propagation laws in the presence and absence of mean flow, and the non-linear interaction of waves with a horizontal mean shear. The first two of these are given a theoretical treatment in Lamb (1932), the last one has been investigated theoretically by J. Drent (1959).

The analysis given by Drent is for the case of plane, long-crested waves and rectilinear shear flow in the absence of surface tension and viscosity. The results indicate that there are two major causes of amplitude change as the waves traverse the flow: one is due to the refraction of the waves, causing a spreading or concentration of energy; and the other is due to the radiation pressure, associated with the waves, interacting directly with the shear flow. For waves running directly into a converging flow these two effects are about equal; for waves crossing a lateral shear at an angle the former appears to be 2 to 3 times larger than the latter. Previous theories have consistently neglected the direct interaction effects. For example, see

Johnson (1947).

This thesis is a report of a laboratory experiment designed to measure the three properties listed above and a comparison of the results with the respective theoretical predictions. The wave energy measurements in the presence of mean flow are compared with two theoretical models - one including the interaction effects, following Drent, and the other omitting the interaction effects following the previous theories.

EXPERIMENTAL METHODS

1. FLOW PRODUCTION

A stable Couette-type flow is created between the outer wall of a circular tank slightly greater than 2.5 meters in diameter and an inner wall imposed by a raised centre portion 1.52 meters in diameter, (see figures 1, 2 for two different views of the actual apparatus and figure 3 for a scale diagram). A hollow annular ring, 2.44 meters in diameter, floats freely, concentric with and about 2.5 cm. radially inside the outer wall of the circular tank (figures 1, 2, point A). A series of six drive jets are situated in the outer wall of the tank and are connected by rubber hoses to the water mains (figures 1, 2, point B). These jets are oriented so that water passing through them impinges on the wall of the annular ring at an angle of 145°, thereby making it rotate. In order to keep the annular ring rotating

about the centre of the tank, three foam-padded castors, spring-mounted, are situated on the wall of the tank and bear gently on the outside of the rotating ring if it is not in the centre of the system (figures 1, 2, point C). It is found that if these castors are not used the ring gradually shifts its axis of rotation until it hits the wall of the tank, creating a large disturbance on the surface of the water. It was necessary to construct a wooden form to fit snugly around the annular ring in order to hold it to a circular shape (figures 1, 2, point D). With the wooden form, the annular ring is circular to within 0.6 cm. in its 2.44 meter diameter.

2. FLOW MEASUREMENT

(i) Primary flow

Measurement of the horizontal shear flow profiles is performed photographically during the experiment in the following way: ten small circular pieces of white paper, 0.6 cm. in diameter, are simultaneously dropped onto the surface of the water in a line approximately at right angles to the flow in the area under consideration. A photograph is taken of these with the camera shutter open for .98 seconds (1 second on camera settings). The lengths of the resulting streaks on the film are proportional to the velocities at the points where the pieces of paper dropped. This is done ten times in order to achieve a smooth profile curve. An example is shown in figure 6.

Depth profiles were obtained with a midget propellor type current meter at three positions radially across the shear flow. However, since the waves that are used are only about 2.5 cm. in wave length, it appears that the current meter could not really get near enough to the surface to examine the important region. Visual observations were obtained comparing the flow at a few centimeters depth and the flow right on the surface. A small plastic float about ½ cm. in diameter was attached to a relatively high drag body of about the same dimensions by a piece of thread a few centimeters long. The rate of movement of this unit when placed in the water was found to be not significantly different from the rate of movement of a plastic float by itself at the same radius. Because there is nothing to produce a surface stress except for the negligible effect of the air, there is little reason to believe that a depth-wise velocity gradient should exist. Any such gradient would be associated with secondary flow.

(ii) Secondary flow

The secondary flow generated in the tank manifests itself mainly in changing the curvature of the radial profile (see Theory). For all intents and purposes the value of the secondary flow is negligible, i.e. the fluid particle trajectories are circular on an average. The strength of the secondary flow was estimated by observation of the paths of the floats described above. On an average they tended towards the outer wall of the system but the rate of progression in

this sense was of the order of 1/200 or less of the average current.

3. WAVE PRODUCTION

Because of the limited surface area of the tank it is necessary to use either a wave absorbing system on the walls or to use a pulsed wave train. The former was attempted but soon abandoned in favour of the latter. The energy absorbing device tried was a 'beach' formed by a strip of sheet metal with ends joined to form a truncated cone and attached to the inside of the annular ring at the water level. Unfortunately, the presence of the rotating beach in the water produced a vertical shear of the horizontal velocity because the submerged part of the beach acted as a boundary not in accord with the flow pattern set up by the outer and inner walls of the tank. This vertical shear zone produced more turbulence than could be tolerated, its effects showing up in the form of local surface depressions and horizontal velocity fluctuations and possibly a change in the dissipation rate of the wave energy.

The most serious drawback with the pulse system is that only the first part of the pulse is available from which to obtain data. The part of the shear flow that is used extends from the edge of the inner wall to approximately 20 cm. from the outer wall, so that the reflected wave arrives at the edge of the region under examination in ½ to 1 second.

Therefore a steady state wave pattern must be created in less than ½ second after the pulse has been applied to the wavemaker.

The device used to produce the waves is as follows: (see figure 4) a circular wooden disc with its edge bevelled from 15.2 cm. in diameter to 11.5 cm. in diameter is firmly attached to the cone of a Jensen #B69V elliptical loudspeaker. This assembly is situated on the top of the raised centre piece of the tank in such a way that excursions of the cone are perpendicular to the surface of the water. The disc extends about 1 cm. under the surface. The loudspeaker is electrically connected to a low frequency oscillator via an automatic switch and a matching transformer (see figure 5). The voltage being applied to the wavemaker is continuously monitored by a single beam oscilloscope. The switching rate used is about one per minute with an "on" duration of about ten seconds. This gives ample time to take the necessary data and enables the waves to die out between pulses.

Two of the prime difficulties of wave production by this method arise from lobal pattern and transient modulation characteristics. Asymmetry of the former arises because of the difficulty of properly orienting the wooden disc with respect to the water. It appears that the bottom of the disc should be accurately parallel to the surface of the water and that the motion of the disc should be accurately perpendicular to it. Transient modulation occurs because a

resonant system is being driven by pulses of off-resonance frequency. Even though the wave amplitude on the scope is constant to within 1 per cent. there still is evidence of a transient modulation phenomenon of 2 to 5 per cent. existing in the waves themselves. In order to reduce these modulation effects the wave amplitude measurements were taken at different parts of each pulse. An electronic counter was set up across the oscillator to determine the time interval between the application of the pulse to the loudspeaker and the instant when the amplitude or phase data was taken. A neon bulb was set to flash every fourth cycle of the frequency used. By using one half of the flash interval as a basic time interval change, the time at which the data is taken with respect to the front of the wave pulse is varied by three or four steps over the available time, depending on the frequency used. One third or one quarter of the total data was obtained at each of these time intervals. The reflected waves begin interfering after a time interval of approximately one second after the initial part of the pulse has passed the area in question.

Two methods were employed to measure or control the oscillator frequency. One of the methods applies when the frequency desired is some integral or half-integral fraction of the 60 cps., such as 8 cps., 8.57 cps., 10 cps., etc., taking advantage of the fact that in this geographical area the mains frequency is held very precisely to 60 cps. The

sync. on the scope is set to 'line' and 60 cps. mains is displayed on its face. The sweep frequency is set so that the trace is triggered at the same rate as the desired frequency on the oscillator or a simple multiple of it. The time interval between sweeps is given exactly by the time taken for the mains to display the integral or half-integral number of 60 cps. waves, including the delay time required in order that the triggering always be instigated at the same phase of the 60 cps. The mains signal is now removed and the oscillator output is displayed. The frequency is varied until a stationary one or two cycle pattern is observed, depending on whether the fraction is integral or half-integral. The other method is used when the frequency of the oscillator is already set by some criterion other than convenience of measurement. In this case the sync. on the scope is set to 'internal' and the oscillator output displayed. The sweep frequency is then varied until a conveniently countable number of cycles occurs between triggerings. With a stop watch the sweep rate is then measured as accurately as desired. The oscillator period is given by the sweep period divided by the number of cycles per sweep.

An attempt to use plane waves was undertaken but it failed because of the end effects of the oscillating rod. Two loudspeakers, spaced apart by a straight glass tube rigidly attached to their cones were used; however, even with a tube 1.52 meters long, the diffraction effects were too large.

4. WAVE MEASUREMENT

An optical system was chosen to measure the wave amplitudes, wave-number and wave direction. A board containing sixty-four light bulbs, #43, is fastened to the ceiling so that the light from these effective point sources reflects off the area of the shear flow to be studied into a properly oriented camera. The lights are in a square array, each 7.6 cm. apart. The board is approximately 3 meters vertically above the surface of the water and approximately 3 meters horizontally from the reflection points on the surface of the water (figure 3). The camera that is used is a 35 mm. Agfa colorflex. It is positioned approximately 1 meter vertically and horizontally from the reflection points on the water surface and angled so that the image of the 'light board' appears in the centre of its field of view.

(i) Amplitude

As the waves cross the image of the board, the image of a light undergoes oscillatory excursions, the maximum of which is a direct measure of the maximum wave slope at the position on the surface of the water from which the undeviated light reflects. The camera shutter is opened for somewhat longer than one wave-period. A grid of streaks is thus obtained on the film, whose lengths are a measure of the maximum excursions of the images of the lights. A small alignment mirror mounted just above the surface of the water and to one side of the image of the light board is oriented to reflect one column of lights into the camera, thus pro-

ducing a constant reference line from frame to frame. (Examples of these photographs are given in figure 6.)

(ii) Wave number

The light board also has twenty-three straight, white nylon strings mounted on it, each in a vertical plane (figure 3). These strings are photographed, utilizing an electronic flash unit. (Examples of these photographs are shown in figure 6.) This enables lines of constant phase to be determined, from which the wave number is measured as a function of position on the shear flow. The flash unit is positioned about 45 cm. from and slightly below the board for half the phase pictures and 30 cm. in front of the centre of the board for the other half of the phase pictures. This ensures measurability of the phases over the whole area of the board. It is necessary to use the smallest aperture stop that is available on the camera because the surface reflecting the light being photographed is locally curved. A bundle of rays of light emanating from a point on the board, reflecting off the wavy surface and into the camera lens, becomes de-focussed or extra heavily concentrated depending on the curvature at the point of reflection. For all aperture stops larger than f/22 this effect makes determination of constant phase lines impossible.

As the waves cross the area in question, the images of the strings are distorted into sinusoids. The procedure for determining the lines of constant phase from

a photograph of this nature is as follows: a photograph is first taken of the string with no surface waves in the area, then photographs are taken when waves are present. When the first photograph is projected, the images of the straight strings are traced onto a piece of graph paper on the projection board and the images of the lights in the alignment mirror are traced out. Then the photographs with waves are projected onto this same piece of graph paper. When the images of the lights in the alignment mirror correspond with the traced images, the traces of the straight strings form a baseline for each of the sinusoidal string images. The places where the sinusoidal image crosses its baseline are marked. Joining up these marks along wave fronts then produces lines of constant phase.

(iii) Projection system

In order to facilitate measurement of the data on the films, a tilted board projection system is used with the focal length of the projector the same as the focal length of the camera. If the board onto which the film is projected is tilted with respect to the projector, to the same angle that the surface of the water makes with the camera, the measurements obtained correspond directly to the plane of the surface of the water to within a uniform scale factor. Details of the setting up procedure are given under section 5, Experimental parameter.

(iv) Propagation and dissipation

The propagation laws governing the transmission of wave properties in both the presence and absence of flow have been experimentally examined. In the absence of flow it is necessary only to know the surface tension and either the wave number or the frequency to determine the velocities of propagation. In the presence of a known steady state flow it is necessary to invoke geometrical arguments in conjunction with a basic assumption regarding the interaction of the two motions (see Theory).

The surface tension was determined by measuring the height of rise of the water in a capillary tube. The bore of the tube was measured by a travelling microscope.

The rate of dissipation of wave energy by viscosity is changed severely by the presence of a surface film of oil or other immiscible fluid material. Because of the inability to include theoretically the effect of this film, a siphon was set up to continuously remove the surface fluid. For purposes of determining the kinematic viscosity of the water, the surface temperature was measured before and after each experiment. The values used were taken from the 'Handbook of Physics and Chemistry'.

In order to measure the rate of dissipation of energy in the absence of any surface films or flow, the camera was moved back and up from the tank in order to spread

the reflection points of the lights apart as much as possible and to move the location of the reflection points to a region where the time between the arrivals of the direct wave pulse and the reflected wave pulse was a maximum. To further reduce the effect of the reflected information, a short beach was placed on the annular ring at the position from which the first reflected energy arrived.

A series of photographs of wave amplitudes were taken at 8 cps., 8.57 cps., and 10 cps., these frequencies possessing wave-numbers representative of those measured in the presence of flow. The photographs were taken about five seconds after the initial part of the wave pulse had begun to affect the images of the lights, thus minimizing transient modulation effects.

5. EXPERIMENTAL PARAMETERS

In order to compute the wave characteristics from the measured values on the film, it is necessary to know the vertical and horizontal distance from each light to its reflection point, of each reflection point from the entrance pupil point of the camera, the angle to which the projection board must be tilted, and the uniform projection scale factor. The distances were all measured by triangulation with a surveying transit. A piece of graph paper was firmly glued onto a pane of glass and the whole assembly held about ¼ cm. under the water surface in the area of the reflection points and

such that the plane of the graph paper was parallel to the surface. With the help of the transit, the graph paper was situated so that one of its ruled lines fell in the vertical plane determined by the camera entrance pupil point and the centre of the tank. A photograph was taken of the images of the lights superimposed on the graph paper. The transit was now used to measure the distances from each light, from the centre of the tank, and from the camera entrance pupil point, to a point on the graph paper previously marked. This photograph, together with these measurements, now serves as a calibration unit from which the projection system is set up properly, its scale factor determined and all the other necessary parameters obtained.

The one second camera shutter speed was accurately measured by photographing the trace on the oscilloscope after the sweep had been calibrated. The sweep rate was determined from the oscillator after the oscillator was adjusted in conjunction with the 60 cps., as explained above. The flash connections on the camera were used to short a small steady voltage onto the vertical input of the scope while the camera shutter was open.

THEORY

1. INTERACTION DYNAMICS

Consider the Navier-Stokes equations in cylindrical polar coördinates for an incompressible fluid:

u_T = total velocity in radial sense

v_T = total velocity in angular sense

w_T = total velocity in vertical sense

p_T = total pressure

r = radius from centre of system

θ = angle measured about centre.

$$\frac{\partial u_T}{\partial t} + u_T\frac{\partial u_T}{\partial r} + \frac{v_T}{r}\frac{\partial u_T}{\partial \theta} + w_T\frac{\partial u_T}{\partial z} - \frac{v_T^2}{r} = -\frac{1}{\rho}\frac{\partial p_T}{\partial r} + \nu\left(\nabla^2 u_T - \frac{u_T}{r^2} - 2\frac{\partial v_T}{r^2\partial\theta}\right) \quad (1a)$$

$$\frac{\partial v_T}{\partial t} + u_T\frac{\partial v_T}{\partial r} + \frac{v_T}{r}\frac{\partial v_T}{\partial \theta} + w_T\frac{\partial v_T}{\partial z} + \frac{v_T u_T}{r} = -\frac{1}{\rho r}\frac{\partial p_T}{\partial \theta} + \nu\left(\nabla^2 v_T - \frac{v_T}{r^2} + \frac{2\partial u_T}{r^2\partial\theta}\right) \quad (1b)$$

$$\frac{\partial w_T}{\partial t} + u_T\frac{\partial w_T}{\partial r} + \frac{v_T}{r}\frac{\partial w_T}{\partial \theta} + w_T\frac{\partial w_T}{\partial z} = -\frac{1}{\rho}\frac{\partial p_T}{\partial z} + \nu\nabla^2 w_T \quad (1c)$$

ρ = density

$$\nabla^2 \equiv \frac{\partial^2}{\partial r^2} + \frac{1}{r}\frac{\partial}{\partial r} + \frac{\partial^2}{r^2\partial\theta^2} + \frac{\partial^2}{\partial z^2}$$

$\nu \equiv$ kinematic viscosity.

For the experimental set-up neglecting secondary flow,

u_T = u, particle velocity due to wave action,

v_T = v + V, particle velocity due to wave action plus current

w_T = w, particle velocity due to wave action

p_T = p + P, fluctuating pressure due to wave action and mean pressure due to mean flow and hydrostatic head.

The centre of the coördinate system is placed at the centre of the tank.

The viscous terms are assumed to have no inter-

action with the non-linear terms, i.e. the viscosity acts to damp out the waves in the same manner as if no mean flow were present, and it is the agency which makes the shear flow of this type possible.

Substituting velocity components and multiplying each equation by its respective velocity component,

$$u\frac{\partial u}{\partial t} + u^2\frac{\partial u}{\partial r} + \frac{u(v+V)}{r}\frac{\partial u}{\partial \theta} + uw\frac{\partial u}{\partial z} - \frac{u(v+V)^2}{r} = -\frac{u}{\rho}\frac{\partial (P+p)}{\partial r} + \text{viscous} \tag{2a}$$

$$(v+V)\frac{\partial v}{\partial t} + (v+V)u\frac{\partial (v+V)}{\partial r} + \frac{(v+V)^2}{r}\frac{\partial v}{\partial \theta} + (v+V)w\frac{\partial v}{\partial z} + \frac{u(v+V)}{r} = -\frac{(v+V)}{\rho r}\frac{\partial (P+p)}{\partial \theta} + \text{viscous} \tag{2b}$$

$$w\frac{\partial w}{\partial t} + wu\frac{\partial w}{\partial r} + \frac{w(v+V)}{r}\frac{\partial w}{\partial \theta} + w^2\frac{\partial w}{\partial z} = -\frac{w}{\rho}\frac{\partial (P+p)}{\partial z} + \text{viscous} \tag{2c}$$

Addition results in:

$$\frac{1}{2}\frac{\partial q^2}{\partial t} + \frac{u}{2}\frac{\partial q^2}{\partial r} + \frac{v}{2r}\frac{\partial q^2}{\partial \theta} + \frac{w}{2}\frac{\partial q^2}{\partial z} + \frac{V}{2r}\frac{\partial q^2}{\partial \theta}$$

$$+ uv\left(\frac{\partial V}{\partial r} - \frac{V}{r}\right) + \frac{uvV}{r} + V\frac{\partial v}{\partial t} + Vu\frac{\partial v}{\partial r}$$

$$+ Vu\frac{\partial V}{\partial r} + \frac{vV}{r}\frac{\partial v}{\partial \theta} + \frac{V^2}{r}\frac{\partial v}{\partial \theta} + Vw\frac{\partial v}{\partial z} =$$

$$-\frac{1}{\rho}\left\{u\frac{\partial}{\partial r} + (v+V)\frac{\partial}{r\partial \theta} + w\frac{\partial}{\partial z}\right\}(P+p) + \text{viscous} \tag{3}$$

where $q^2 \equiv u^2 + v^2 + w^2$.

Now integrate from bottom of tank, i.e. $-\infty$, to surface of the water, $+\zeta$, where ζ is the variable describing

the surface elevation under influence of the waves.

$$\frac{\partial}{\partial t}\text{(kinetic energy of waves)} + \text{(transport of kinetic energy due to fluctuating velocities)} + \frac{V}{r}\frac{\partial K.E.}{\partial \theta}$$

$$+\int_{-\infty}^{\zeta} uv\left(\frac{\partial V}{\partial r}-\frac{V}{r}\right)dz + \frac{V}{r}\int_{-\infty}^{\zeta} uv\,dz + \int_{-\infty}^{\zeta}\left\{V\frac{\partial v}{\partial t} + Vu\frac{\partial v}{\partial r} + uV\frac{\partial V}{\partial r}\right.$$

$$\left.+\frac{vV}{r}\frac{\partial v}{\partial \theta} + \frac{V^2}{r}\frac{\partial v}{\partial \theta} + Vw\frac{\partial v}{\partial z}\right\}dz = -\frac{1}{\rho}\int_{-\infty}^{\zeta}\left\{u\frac{\partial}{\partial r} + \frac{v}{r}\frac{\partial}{\partial \theta} + w\frac{\partial}{\partial z}\right\}\{P+p\}\,dz$$

$$-\frac{V}{\rho r}\int_{-\infty}^{\zeta}\frac{\partial p}{\partial \theta}\,dz - \frac{V}{\rho r}\int_{-\infty}^{\zeta}\frac{\partial p}{\partial \theta}\,dz + \text{viscous} \qquad (4)$$

In considering the orders of magnitude of the various terms it is seen that for very small waves, i.e. p, u, v, w, ζ, small compared to V and P, the terms become divided into first order, second order and third order terms. It will be seen presently that all first order terms will cancel so considerations will be taken to second order. All third order terms shall be considered negligible in the present treatment. Therefore the upper limit of integration when applied to second order terms will be set to zero, the wave-free surface level, since the remainder is a third order term. All first order terms when integrated remain sinusoidal in nature. Under these considerations the equations are now averaged with respect to time over a large number of waves and a steady state assumed.

To second order:

$$\frac{V}{r}\frac{\partial K.E.}{\partial \theta} + \overline{\int_{-\infty}^{0} uv\left(\frac{\partial V}{\partial r} - \frac{V}{r}\right) dz} + \frac{V}{r}\overline{\int_{-\infty}^{0} uv\, dz}$$

$$+ \overline{\int_{-\infty}^{0} \left\{ Vu\frac{\partial v}{\partial r} + \frac{Vv}{r}\frac{\partial v}{\partial \theta} + Vw\frac{\partial v}{\partial z} \right\} dz} = -\frac{V}{\rho r}\overline{\int_{-\infty}^{0} \frac{\partial p}{\partial \theta} dz}$$

$$- \frac{1}{\rho}\left\{ \frac{1}{r}\frac{\partial}{\partial r} r \overline{\int_{-\infty}^{0} pu\, dz} + \frac{1}{r}\frac{\partial}{\partial \theta}\overline{\int_{-\infty}^{0} pv\, dz} \right\} + \frac{1}{r}\frac{\partial}{\partial \theta}\overline{\int_{-\infty}^{\zeta} p V dz}$$

+ viscous (5)

employing the continuity condition

$$\frac{\partial u}{\partial r} + \frac{1}{r}\frac{\partial v}{\partial \theta} + \frac{\partial w}{\partial z} = -\frac{u}{r} \qquad (6)$$

and where the bar indicates the average with respect to time. However, by the equation of mean motion of the v component it is seen that

$$-\frac{V}{\rho r}\overline{\int_{-\infty}^{0} \frac{\partial p}{\partial \theta} dz} = \frac{V}{r}\overline{\int_{-\infty}^{0} uv\, dz} + V\overline{\int_{-\infty}^{0} w\frac{\partial v}{\partial z} dz} + \frac{V}{r}\overline{\int_{-\infty}^{0} v\frac{\partial v}{\partial \theta} dz}$$

$$+ V\overline{\int_{-\infty}^{0} u\frac{\partial v}{\partial r} dz} \qquad (7)$$

Therefore,

$$-\frac{1}{\rho}\left\{ \frac{1}{r}\frac{\partial}{\partial r} r \overline{\int_{-\infty}^{0} pu\, dz} + \frac{1}{r}\frac{\partial}{\partial \theta}\overline{\int_{-\infty}^{0} pv\, dz} \right\} - \frac{V}{r}\frac{\partial}{\partial \theta}\overline{\int_{-\infty}^{0} \frac{1}{2} q^2 dz}$$

$$- \frac{V}{r}\overline{\int_{-\infty}^{\zeta} p\, dz} = \left(\frac{\partial V}{\partial r} - \frac{V}{r}\right)\overline{\int_{-\infty}^{0} uv\, dz} - \text{viscous} \qquad (8)$$

It is assumed that the local wave properties are given by an irrotational velocity potential, or, the local change of the character of the wave motion is felt at higher than second order so that an irrotational wave model may still be employed to this approximation.

If the velocity potential with respect to the moving fluid is given by φ, Bernoulli's theorem in the absence of viscosity produces:

$$\frac{p_T}{\rho} = \frac{\partial \varphi}{\partial t} - gz - \tfrac{1}{2}q^2 + \text{const.} \tag{9a}$$

or,

$$\frac{p}{\rho} = \frac{\partial \varphi}{\partial t} - g(z - \bar{z}) \tag{9b}$$

Thus, the last term on the left hand side of equation (8) becomes $-\frac{V}{r}\frac{\partial}{\partial \theta}$(potential energy per unit surface area of wave motion), which, combined with the second to last term, becomes $-\frac{V}{r}\frac{\partial}{\partial \theta}$ (total energy per unit area of wave motion). The first term becomes the negative of the divergence of the total power represented by the wave motion plus third order terms, representing the transport of the wave potential energy by the fluctuating motions. Thus, the terms on the left side combine to form the negative of the divergence of the total power of the waves, as determined by an observer stationary with respect to the coördinate system. The right side of the equation becomes

$$-\frac{E}{4}\sin 2(\alpha + \theta)\left(\frac{dv}{dr} - \frac{v}{r}\right)$$

where α is the angle between the arbitrary zero angle direction and the normal to the wave front at the point in

question. The angle α is considered positive if measured in a clockwise sense; the angle θ is considered positive if measured in a counter-clockwise sense (see figure 8). Since the total energy of a wave group is propagated by wave action at the group velocity, $\underline{c}$, the final equation can be written most simply in vector form as follows:

$$\text{div } E(\vec{\underline{c}} + \vec{V}) = \frac{1}{4}E\sin 2(\alpha + \theta)\left(\frac{dV}{dr} - \frac{V}{r}\right) - \text{viscous} \qquad (10)$$

where $\vec{\underline{c}}$ is in the direction of advance of the wave and normal to its front, and $\vec{V}$ is tangential to the mean streamline and in the direction of positive θ.

The path obtained by integrating from the inner edge of the flow outwards with the direction of $\vec{\underline{c}} + \vec{V}$, a function of r and θ , tangent at every point to the path shall be called a "group ray". A path line defined this way possesses the property that no wave energy crosses it. That is, given any two group rays, the rate that energy flows across any line joining these rays is the same as the rate that energy flows across any other line joining them in the absence of dissipating mechanisms and non-linear interactions. Therefore, by considering the configuration of the group lines on the water surface the effect of the refraction and spreading of energy can be taken into account.

Equation (10) can be reduced to simpler terms by integrating it over the area contained between two differentially separated group rays and any two arbitrary points on the rays:

$$E_2\left|\vec{c}+\vec{V}\right|_2 \ell_2 - E_1\left|\vec{c}+\vec{V}\right|_1 \ell_1 = \frac{1}{4}\iint_1^2 E\sin 2(\alpha+\theta)\left(\frac{dV}{dr}-\frac{V}{r}\right)d\ell\, ds - \text{viscous} \qquad (11)$$

or

$$\frac{\Delta\left(E\left|\vec{c}+\vec{V}\right|\ell\right)}{\ell\,\Delta s} = \frac{1}{4}E\sin 2(\alpha+\theta)\left(\frac{dV}{dr}-\frac{V}{r}\right) - \text{viscous} \qquad (12)$$

where ℓ is the perpendicular distance separating the two group rays and ΔS is an element of length along the group rays.

The theoretical curves used for comparison purpose with the experimentally determined data have been obtained by a numerical integration of the equation (3) including viscosity, along a previously determined group ray: the interaction curve including the term $\frac{1}{4}E\sin 2(\alpha+\theta)\left(\frac{dV}{dr}-\frac{V}{r}\right)$, the non-interaction curve omitting it.

2. VISCOUS DISSIPATION

The viscous decay term that has been used in the determination of the above-mentioned theoretical curves is essentially the same as that given in Lamb (1932, #348, 349). If the assumption is made that irrotational waves maintain their irrotationality even though decaying by means of a rotational agency, the rate of energy decay is given by:

$$\frac{dE}{dt} = -E(4\nu k^2)$$

where k is the instantaneous wave number. By considering only a group ray again, it is possible to change the time derivative to a spatial derivative by the following trans-

formation:

$$\frac{d}{dt} = \left| \vec{c} + \vec{V} \right| \frac{d}{ds} \tag{13a}$$

Therefore, $$\frac{dE}{ds} = - E \frac{4\nu k^2}{\left| \vec{c} + \vec{V} \right|} \tag{13b}$$

(For a partial justification of this equation experimentally, see Results - Viscous decay.)

3. WAVE KINEMATICS

In figure 9, part 1, A and B are two consecutive crests. For the condition of a steady state, the point E traverses to point F in the same time that the point C traverses to point D.

Therefore, $$\frac{1}{f_o} = \frac{\lambda}{c - V\sin(\alpha+\theta)} \tag{14a}$$

where f_o is the frequency of the oscillations of the wave-maker, λ is the wavelength of the wave at G, defined as the minimum distance between consecutive crests, and C is the phase velocity of the wave relative to the water.

Thus, using $k = \frac{2\pi}{\lambda}$, $\omega_o = 2\pi f_o$

$$kc - \omega_o = kV\sin(\alpha+\theta) \tag{14b}$$

(i) Zero'th Order Approximation

(See figure 9, part 2.) Clearly, if all wave crests make the same angle with respect to the shear flow when entering the region of flow, then whatever happens to one wave crest will precisely happen to its neighbours

except for a constant angle of rotation about the tank centre. The trajectory of a wave crest shall be called a PHASE RAY and is defined in the same way as a group ray except that the phase velocity is used in place of the group velocity. The tank centre, to this approximation, is a point of isotropy with respect to these phase rays.

It can be seen that the distance along arc A between the two crests is given by $r_o\beta$, thus

$$\lambda_o = r_o\beta \sin(\alpha+\theta)_o \qquad (15)$$

For steady state, when these two crests reach arc B the distance separating them along B is $r\beta$, thus

$$\lambda = r\beta \sin(\alpha+\theta)$$

therefore, using $k = \frac{2\pi}{\lambda}$

$$kr\sin(\alpha+\theta) = \text{const.} \qquad (16)$$

This approximation becomes exact for the phase ray which joins the wavemaker at a right angle with respect to the line between the wavemaker and the tank centre. Thus, the constant in equation (16) is equal to k_oL, where k_o is the wave-number in the absence of flow and L is the distance from tank centre to wavemaker.

From equations (14b) and (16) it is possible to eliminate $(\alpha+\theta)$, leaving k as a function of r only.

$$kc - \omega_o = \frac{k_o VL}{r} \qquad (17)$$

$$\text{using } C = \sqrt{\frac{g}{k} + \frac{kT}{\rho}} \tag{18}$$

(Lamb, 1932, #267) where T is the surface tension of the water and g is the acceleration of gravity; and, using V as measured, values of k have been determined and are compared with measured values.

In order to determine the rate of spreading of the energy, i.e. ℓ defined in equation (12) as a function of r, employing zero'th order theory, it is only necessary to use the fact that all the group rays are geometrically similar with respect to the tank centre. If the distance along an arc about the tank centre between two group rays at the edge of the flow is $d_o = r_o \psi$ then the separation between these same rays, measured along an arc about the tank centre, at any radius r is $d = r\psi$ but, $\ell = d \cos(\varphi_G + \theta)$ where φ_G is the angle that the tangent to the group ray makes with the arbitrarily chosen zero angle line.

Therefore, $$\ell = \ell_o \frac{r}{r_o} \frac{\cos(\varphi_G + \theta)}{\cos(\varphi_G + \theta)_o} \tag{19}$$

(ii) First Order Theory

In order to reduce the errors introduced by the use of zero'th order theory, a first order theory has been devised. It is convenient to consider the total rate of energy transport between a real group ray and an artificial one constructed by rotating the real one about the tank centre by a differential angle $\Delta\theta$. If this second ray is in

fact a real group ray, zero'th order spreading applies. If the second ray is not a real group ray, the first order effect can be obtained by determining how much energy actually flows across a line drawn perpendicularly between the two rays at an arbitrary radius compared with how much would flow across the same line on the basis of zero'th order theory, in the absence of viscosity and interaction.

The total rate of propagation of energy can be resolved into two perpendicular components: one along the radius at the point in question and the other at right angles to it. The former component is given by $E\underline{c}\cos(\alpha+\theta)$ with dimensions of energy per unit time per unit arc length, the latter is given by $E(\underline{c}\sin(\alpha+\theta) - V)$ with dimensions of energy per unit time per unit radial length. The following discussion of the group rays proceeds assuming ray I at the left of ray II with the current and increasing θ in the direction from I to II. Given that $(\alpha+\theta)_1$ is the angle that the normal to the wave front makes with the radius at a given radius on ray I, then

$$(\alpha+\theta)_2 = (\alpha+\theta)_1 + \frac{\partial(\alpha+\theta)}{\partial\theta}\Delta\theta \qquad (20)$$

is the angle that the wave crest normal makes with the radius at the same radius on ray II to first order. The effect of the dependence of $(\alpha+\theta)$ on θ is made evident by the rate at which energy is actually crossing ray II. This rate is given by $E\underline{c}\{\sin(\alpha+\theta)_2 - \sin(\alpha+\theta)_1\}$, or

$$\text{Excess rate of flow of energy between rays I and II per unit time per unit radial length} = E\underline{c}\,\frac{\partial(\alpha+\theta)}{\partial\theta}\Delta\theta\cos(\alpha+\theta) \tag{21}$$

Therefore, since $\Delta r = \Delta s\cos(\varphi_G + \theta)$, where s is distance measured along a group ray,

$$\text{Excess energy flowing per unit time between the two rays} = \int_{s_o}^{s} E\underline{c}\cos(\alpha+\theta)\cos(\varphi_G+\theta)\frac{\partial(\alpha+\theta)}{\partial\theta}\Delta\theta\,ds \tag{22}$$

The rate at which energy flows across a line drawn perpendicularly between these two rays at r_o is given by

$$E_o\left|\vec{\underline{c}} + \vec{V}\right|_o r_o\cos(\varphi_G+\theta)_o\Delta\theta.$$

Thus, in the absence of any dissipation or production of energy, the rate of flow of energy across a perpendicular between these rays at any other point will satisfy the equation

$$\begin{aligned} E\left|\vec{\underline{c}}+\vec{V}\right| r\cos(\varphi_G+\theta) &= E_o\left|\vec{\underline{c}}+\vec{V}\right|_o r_o\cos(\varphi_G+\theta)_o \\ &\quad + \int_{s_o}^{s} E\underline{c}\cos(\alpha+\theta)\cos(\varphi_G+\theta)\frac{\partial(\alpha+\theta)}{\partial\theta}ds \\ &= E_o\left|\vec{\underline{c}}+\vec{V}\right|_o r_o\cos(\varphi_G+\theta)_o\left\{1\right. \\ &\quad \left. + \frac{1}{r_o}\int_{s_o}^{s}\frac{E\underline{c}\cos(\alpha+\theta)}{E_o\underline{c}_o\cos(\alpha+\theta)_o}\cos(\varphi_G+\theta)\frac{\partial(\alpha+\theta)}{\partial\theta}ds\right. \end{aligned} \tag{23}$$

Between any two real group rays it can be seen from equation (12) that $E\left|\vec{\underline{c}} + \vec{V}\right|\ell$ is a constant in the absence of dissipation or interaction. Equation (23), then, may be taken as defining ℓ as a function of r if, except for $\frac{\partial(\alpha+\theta)}{\partial\theta}$, zero'th order values are used to evaluate the integral. In this case,

$$\ell = \ell_o \frac{r\cos(\varphi_G + \theta)}{r_o \cos(\varphi_G + \theta)_o} \left\{ 1 + \frac{1}{r_o} \int_{S_o}^{S} \frac{Ec\cos(\alpha + \theta)}{E_o c_o \cos(\alpha + \theta)_o} \frac{\partial(\alpha + \theta)}{\partial \theta} \cos(\varphi_G + \theta) ds \right\}^{-1} \qquad (24)$$

In order to determine the necessary values of $\frac{\partial(\alpha + \theta)}{\partial \theta}$ it is assumed to be constant along any given phase line, thus it has the value at any point given by its evaluation at the location where the phase ray that goes through that point enters the region of flow. In the zero'th order case this assumption is exactly true since $\frac{\partial(\alpha + \theta)}{\partial \theta}$ is everywhere zero. It is assumed, therefore, that variations of $\frac{\partial(\alpha + \theta)}{\partial \theta}$ along a phase ray will exist only to first order compared with its value. Evaluation is obtained from the following equations:

In the absence of flow (figure 7),

$$r\sin(\alpha + \theta) = L\sin(\alpha + \gamma) \qquad (25)$$

From which is obtained

$$\frac{\partial(\alpha + \theta)}{\partial \theta} = \frac{\tan(\alpha + \theta)}{\tan(\alpha + \theta) - \tan(\alpha + \gamma)} \qquad (26)$$

Equations (24), (25) and (26) permit calculation of the first order spreading. As will be seen (page 37), the difference between the zero'th and the first order spreading is so small that higher orders need not be considered.

4. SECONDARY FLOW

The mean flow generated by the tank system includes a secondary flow because of the proximity of the bottom. If the vertical component of the secondary flow is assumed not important compared to the radial component in regions near

the surface and not too near either wall, the equation

$$U\frac{dv}{dr} + \frac{Uv}{r} = \nu\left(\frac{d^2v}{dr^2} + \frac{1}{r}\frac{dv}{dr} - \frac{v}{r^2}\right) \qquad (27)$$

represents the flow very closely, with U as the radial component, V as the angular component and ν as the kinematic viscosity. Total derivatives are used because under these assumptions V is a function of the radius only.

For a region not too near the walls and at the surface the functional form of U that has been chosen in order to solve equation (27) is a source-like one, i.e. $U = \frac{A}{r}$ where A is an as yet unevaluated constant. Equation (27) now has a solution given by

$$V = B\left(r^n - \frac{r_o^{n+1}}{r}\right) \qquad (28)$$

with r_o as the radius of the inner wall and $n = 1 + \frac{A}{\nu}$. It is interesting to note that the curvature in equation (28) changes from negative to positive for $r > r_o$ with a change of n from 1 to 2: that is, a secondary flow changing from zero to $\frac{\nu}{r}$. The value of $\frac{\nu}{r}$ for $r \simeq 1.0$ meters is about 10^{-4} cm./sec. This is negligible in terms of interaction phenomena yet it changes the position of maximum $\frac{dv}{dr} - \frac{v}{r}$ from near the inner wall to near the outer wall, and by equation (3) the position where this is maximum is also the position of maximum interaction.

5. ANALYSIS OF AMPLITUDE PHOTOGRAPHS

The theory used to obtain the equations which relate

streak lengths on the film to actual wave slopes is given in the Appendix. It is possible to determine exact relationships but for the purpose of analysis, modified linear equations were used. The errors introduced by linearization are less than 1 per cent. for waves of the size used ($\sim$.008 cm. in amplitude). Since absolute wave amplitudes are never required, the effective error in the final comparison curves will be less than 1 per cent. by a factor of 2 or more.

RESULTS

1. ABSENCE OF FLOW

(i) Propagation

On the assumptions of irrotationality, incompressibility and infinitesimally small amplitudes, inviscid wave theory produces the result given in equation (18),

$$c = \sqrt{\frac{g}{k} + \frac{kT}{\rho}}$$

and since $\omega = kc$,

$$\omega^2 = gk + \frac{k^3 T}{\rho}$$

For a wave frequency of 8.00 cps. and a surface tension of 67 $\pm$ 4 dynes/cm., this equation yields k = 2.015 cm. $\pm$ .02. In two experimental determinations at 8.00 cps. k was found to be 2.028 cm. $\pm$ .02 and 2.033 cm. $\pm$ .02.

(ii) Viscous dissipation

Results of the viscous dissipation experiments are

presented in graphical form in figure 10. The theoretical curves plotted are taken directly from equation (4) written in terms of amplitudes and with V = 0. A term in $\sqrt{\frac{s}{s_o}}$ is included to account for spreading of energy:

$$\frac{\text{wave slope}}{\text{wave slope}_o} = \sqrt{\frac{s_o}{s}}\; e^{\frac{-2\nu k^2 s}{c}} \qquad (29)$$

The parameters Wave Slope$_o$ and S_o are taken as the average measured wave slope at that particular frequency and the distance from the wavemaker at which that average occurs. Thus, discrepancies from the theory show up when the slopes of the solid lines do not agree with the slopes of the measured points.

The 8 cps. data is seen to agree quite well with the theory except for the wavy characteristic of the measured points. This waviness is thought to be due to the presence of small amounts of reflected energy.

At 8.57 cps. the theoretical line disagrees appreciably with the measured points. The reason for or significance of this result is as yet unknown.

The 10.0 cps. data was taken with the aim of measuring the viscous dissipation of a wave whose phase velocity is exactly the same as that of a wave with twice its frequency. Unfortunately, it appears that this condition has not been achieved. From the photographs used to measure the wave slopes it can be seen that an extra wave train is

present, but in the distance covered by the measurements the phase of this extra wave with respect to the 10.0 cps. wave has changed by 90°. It is thought that the apparently rapid decay over the left side of the graph in figure 10 is a combination of two factors. One is the fact that any wave of a frequency of 20.0 cps. which has appreciable amplitude that far from the wavemaker must have a continuous source of energy as it propagates. One source of energy is a non-linear wave-wave interaction with the fundamental. Between any crest of the fundamental and the preceding trough is a region which is undergoing a continual rate of compression by the fluid particle velocities. If a part of an extra wave happens to coincide with this region for any length of time it will be increased in energy by the same sort of interaction as that between waves and a mean shear. (Longuet-Higgins and Stewart, 1960, "Journal of Fluid Mechanics", in the press.) The larger velocity gradients present in the 20.0 cps. wave result in a much faster decay of energy to viscosity; so, presumably a balance is achieved between non-linear input and viscous decay. The fundamental thus experiences an increased rate of loss of energy. A phase photograph of a wave at 10.5 cps. is given in figure 7, clearly showing the complexity of the wave form.

The other contributing factor to the anomalous measured decay rate of the 10.0 cps. waves is due to the change of phase that occurs between the two types of waves. The

shape of the parts of the wave from which the light reflections take place can be inferred from the character of the streak density obtained from an amplitude photograph. From an examination of this type it appears that the parts of the wave which give the maximum excursions of the reflected light change from having a slope more nearly like that of 20.0 cps. to that characteristic of a 10.0 cps. saw-tooth wave. The peculiarities of waves in the neighbourhood of 10 cps. have been noted previously (Wilton, 1915; Pierson, 1960).

2. PRESENCE OF FLOW

Two complete sets of data were taken in the presence of flow. Set I had an oscillator frequency of 8.23 cps. and a velocity profile as shown in figure 11. Set II had an oscillator frequency of 6.00 cps. and the velocity profile given in figure 14. For both sets of data, one hundred amplitude photographs were taken and the 'best' twenty in each were measured. The criterion used to judge which frames were to be measured was based on overall smoothness of the streak lengths within the frame being judged. (See figure 6 for an example of a photograph rejected on this basis compared with two that were not.) The judgment was a purely visual one, i.e. it was performed before any of the streak lengths were actually measured. These anomalous streak variations are caused by the accumulative effect of fluctuations in the horizontal velocity that occur during the time required for the energy to propagate from the edge of the shear flow to

the position of examination. The major effect of a local velocity fluctuation is a change of the rate of spreading from that point onwards along the group rays affected.

For Set I, a total of forty phase pictures were taken, of which five were chosen and measured. The judgment in this case was visual and was based on the smoothness of the sinusoidal string images. In this case, however, the cause of the discrepancies was due only partially to velocity fluctuations and mostly to the presence of any waves of a period different from the main 8.23 cps. component. Waves of different period exist as is shown by the presence of transient modulation. If any waves of different period do exist they will be refracted differently than the 8.23 cps. wave according to equations (14b) and (16).

For Set II, an attempt was made to take forty photographs but because of a faulty camera aperture mechanism only ten usable ones resulted. On the whole, these ten were much freer from discrepancies than those of Set I, so no difficulty was encountered in choosing five frames.

Figures 17 and 18 contain typical lines of constant phase from sets I and II respectively. Only data from two out of the five frames is shown in each.

(i) Propagation

It can be seen that the values predicted for wave-number on the basis of equation (17) depend on the value of

the phase velocity at that wavenumber. Therefore, a comparison between predicted and measured wavenumbers will determine how accurately equation (18) is obeyed, assuming zero'th order kinematics to hold.

The theoretical curves shown in figures 12 and 15 are plotted from equation (17) and are determined from Set I information and Set II information respectively. The measured points are obtained from the respective 'lines of constant phase' diagrams in the following manner: a series of seven straight lines are drawn on the constant phase diagrams parallel to the zero baseline for angles. They are spaced equally apart and cover all the information. Wavelengths are then measured both forward and backward from all the positions where lines of constant phase cross the seven straight lines, and the respective distances of these positions from the tank centre are determined. The data subsequently used is the average of the forward and backward measurements at any given point. The measured points shown in figures 12 and 15 comprise a non-selective choice of one-fifth of the information obtained along one of the seven lines regarded as typical in each case. This method of presenting the data was chosen in order to show the amount of scatter in the measurements without overcrowding the diagram. Smoothing of the measured points in figure 12 was done visually.

As can be seen from figures 12 and 15, Set II data

agrees very well with equation (7) whereas Set I data differs significantly from it. The maximum discrepancy in figure 12 (approximately 5 per cent.) occurs at $k \simeq 2.7$ cm.$^{-1}$ and, since the wavenumber that propagates at the same phase velocity as the wave at twice the wavenumber has a value of 2.71 cm.$^{-1}$, calculated from equation (18), it is thought that the two phenomena are intimately linked, though exactly how is not yet understood. In order to estimate the maximum error introduced by the use of equation (16), equation (14b) was used to determine that

$$\frac{\partial k}{\partial \theta} \leq .05 \text{ cm.}^{-1}$$

Therefore, since $\Delta\theta$ is less than 0.1 radians measured from the phase line for which the zero'th order theory is exact to the positions at which k was measured, the error in k predicted from equation (17) will be less than .005 cm.$^{-1}$, i.e. negligible.

The only possibility, it seems, is that the value of the phase velocity is in error. If this is so, the propagation speed in the vicinity of $k = 2.7$ cm.$^{-1}$ differ from those obtained on simple theory by approximately 5 per cent.

(ii) Interaction

In order to determine the results of the interaction measurements several calculations must be made. One of the first of these is the determination of a group ray along which equation (12) is to be solved numerically with and

without the interaction term. The group rays that are used were obtained simply from a graphical integration of the equation

$$-\frac{r d\theta}{dr} = \tan(\varphi_G + \theta) \tag{30}$$

or, (see figure 8)

$$-\frac{r d\theta}{dr} = \tan(\alpha + \theta) - \frac{v}{c}\sec(\alpha + \theta) \tag{31}$$

The angle $(\alpha + \theta)$ was in all cases determined from equation (16) using the measured values of k. The group rays so obtained are shown in figures 17 and 18 for sets I and II respectively. (The circles shown in these figures are the positions of reflection of the lights.) Eight wave slopes are then determined for each frame of amplitude photographs chosen to be measured - one for each row of lights. If the group ray happens to pass between two lights, the value of the slope at the ray is obtained by interpolation between the lights. Each frame is then normalized by setting the average wave slope along the group ray for each frame to unity. The normalized measured values for each point on the group ray are then averaged over all twenty frames. The standard errors of each point are then calculated from the normalized data. The final averages for Set I are shown as the measured points in figure 13 with the vertical bars indicating one standard error on each side.

The theoretical curves plotted in figure 13 were calculated on the basis of zero'th order kinematics -

inclusion of first order effects produces a negligible change. They incorporate the smoothed wavenumber data of figure 12 in the conversion of energy to slope. They also are normalized to unity at the same position along the group ray at which the averaged wave slope occurs. The theoretical curves used for Set II incorporated first order spreading theory. The maximum deviation from zero'th order theory encountered was 1.7 per cent. in wave slope. Figure 16a represents the data obtained in Set II, plotted in the same manner as figure 12. The upper points in figure 16b are plotted as the difference between the measured points and the normalized theory omitting the interaction term. The lower points in figure 16b are plotted as the difference including the interaction term. In both cases, the vertical bars indicate one standard error on each side of the points, and the dashed straight line was obtained by least squares regression through the points. The interaction effect results in an added energy change of 12 per cent. over the distance examined. The change in energy due to spreading is about 30 per cent.

DISCUSSION

The optical methods used in this experiment were entirely satisfactory - it is estimated that an accuracy of 0.5 per cent. could be achieved in all the optical measurements if extreme care is exercised.

The method used to create the shear flow, though

extremely simple and adequate, possessed one major drawback - unsteadiness. Because of up-welling at the inner wall, a region of turbulence existed at the edge of the flow. This region produced most of the random variations of wave properties that were subsequently dealt with by statistical analysis.

Considerable time was spent trying to produce waves with very little transient modulation. Unfortunately the problem was not entirely solved. The attempt to randomize the phase of the modulation from pulse to pulse appears to have succeeded for Set I data but not completely for Set II.

It appears that a further experimental investigation is warranted into viscous dissipation and propagation properties of waves near $k = 2.7$ cm.$^{-1}$, both in the presence and absence of mean flow.

The interaction measurements as presented in figure 13 are definitely anomalous. The difference in decay rate between the measured points and the theoretical curves is in the same sense and of approximately the same magnitude as the discrepancies noted in the viscous decay between 8.57 cps. and 10.0 cps. It is perhaps significant that a sudden decay of energy occurs very near the position along the group ray, 12 cm., at which $k = 2.7$ cm.$^{-1}$ occurs.

No anomalies were found in the information taken

in Set II and figures 16a and 16b clearly indicate that interaction theory is well favoured over non-interaction theory.

SUMMARY

Except for the wavenumber region near $k = 2.7$ cm.$^{-1}$, it has been found that:

(a) viscous dissipation is not significantly different from the theoretical predictions given in Lamb (1932);

(b) propagation laws for infinitesimal, inviscid waves are obeyed;

(c) interaction theory taken to second order in wave slope is not significantly different from the measurements, whereas theoretical predictions based on the omittance of the non-linear interaction term are significantly different.

The viscous decay and propagation properties appear to be anomalous for wavenumbers near $k = 2.7$ cm.$^{-1}$.

APPENDIX

Amplitude Analysis

Consider figure 19. Let the point J be situated on the part of a wave whose slope is tan δ . Subsequent analysis will assume that the elevation of point J from the plane GDH is negligible. (For waves of approximately .008 cm. in amplitude, the error of this assumption is of order 10^{-3} per cent.) Thus, by the law of specular reflection, angle AJB = angle BJC. Let ϵ and μ be the angles described by the projection of δ on the planes AGH and AGD respectively. By considering triangles AJC and AEC it can be determined that

$$\frac{\sin\rho}{\sin\chi} = \sqrt{\left(\frac{b^2 + (a - x)^2}{b^2 + (a - x)^2 + y^2}\right)\left(\frac{c^2 + (d + x)^2 + y^2}{c^2 + (d + x)^2}\right)} \qquad (A1)$$

Similarly, by considering triangles AHL and AJC

$$\frac{\sin\tau}{\sin\sigma} = \sqrt{\left(\frac{c^2 + y^2}{b^2 + y^2}\right)\left(\frac{b^2 + a^2 + y^2}{c^2 + d^2 + y^2}\right)} \qquad (A2)$$

Using maximum values for x and y and measured values for a, b, c, d:

$$\sin\rho = .99935 \sin\kappa$$

$$\sin\tau = .99994 \sin\sigma$$

therefore, $\rho = \kappa$, $\tau = \sigma$, with an error of less than .1 per cent.

Let angle AEG = λ , angle CED = ν .

Thus, $$\nu + \kappa - \mu = \lambda + \rho + \mu \qquad (A3)$$

or $$2\mu = \nu - \lambda \qquad (A4)$$

Similarly, let angle AHG = γ , angle LHG = β

then, $$\pi - \gamma - \epsilon + \sigma = \beta + \epsilon + \tau \qquad (A5)$$

or $$2\epsilon = \pi - \gamma - \beta \qquad (A6)$$

Now, $\tan \nu = \dfrac{b}{a - x}$

and $\tan \lambda = \dfrac{c}{d + x}$

therefore, $\tan 2\mu = \dfrac{b(d + x) - c(a - x)}{(a - x)(d + x) + bc}$

or $$\tan 2\mu = \frac{(b + c)x}{ad + bc + (a - d)x - x^2} \qquad (A7)$$

Also, $\tan\gamma = \dfrac{c}{y}$ and $\tan\beta = \dfrac{b}{y}$

Therefore $$\tan 2\epsilon = \frac{(b + c)y}{bc - y^2} \qquad (A8)$$

Tan δ is obtained from equations (A8) and (A7) as follows:

$$\tan^2\delta = \tan^2\mu + \tan^2\epsilon \qquad (A9)$$

The actual measurements indicate that equations (A7) and (A8) can be linearized with a maximum error of approximately .7 per cent. Therefore:

$$\tan\mu = \frac{(b + c)}{2(ad + bc)}\, x \qquad (A10)$$

$$\tan\epsilon = \frac{(b + c)}{2bc}\, y \qquad (A11)$$

If the measured values of x and y are taken as the components of the total length of the streak an additional factor of 2 must be incorporated in the denominators in equations (A10) and (A11).

BIBLIOGRAPHY

Drent, J., 1959, "A Study of Waves in the Open Ocean and of Waves on Shear Currents", Doctoral Thesis, University of British Columbia.

Handbook of Physics and Chemistry, 41st edition.

Johnson, J.W., 1947, Trans. American Geophysical Union, Vol. 28, No. 6.

Lamb, H., 1932, Hydrodynamics, 6th ed., Cambridge University Press.

Longuet-Higgins, M., and Stewart, R.W., 1960, J. Fluid Mech., in the press.

Pierson, W.J., and Fife, P., 1960, "Some Properties of Long Crested Periodic Waves with Lengths near 2.44 Centimeters", Technical Report, Dept. of Meteorology and Oceanography, Research Div., College of Engineering, New York University.

Wilton, J.R., 1915, Philosophical Magazine, Vol. 29, Ser. 6.

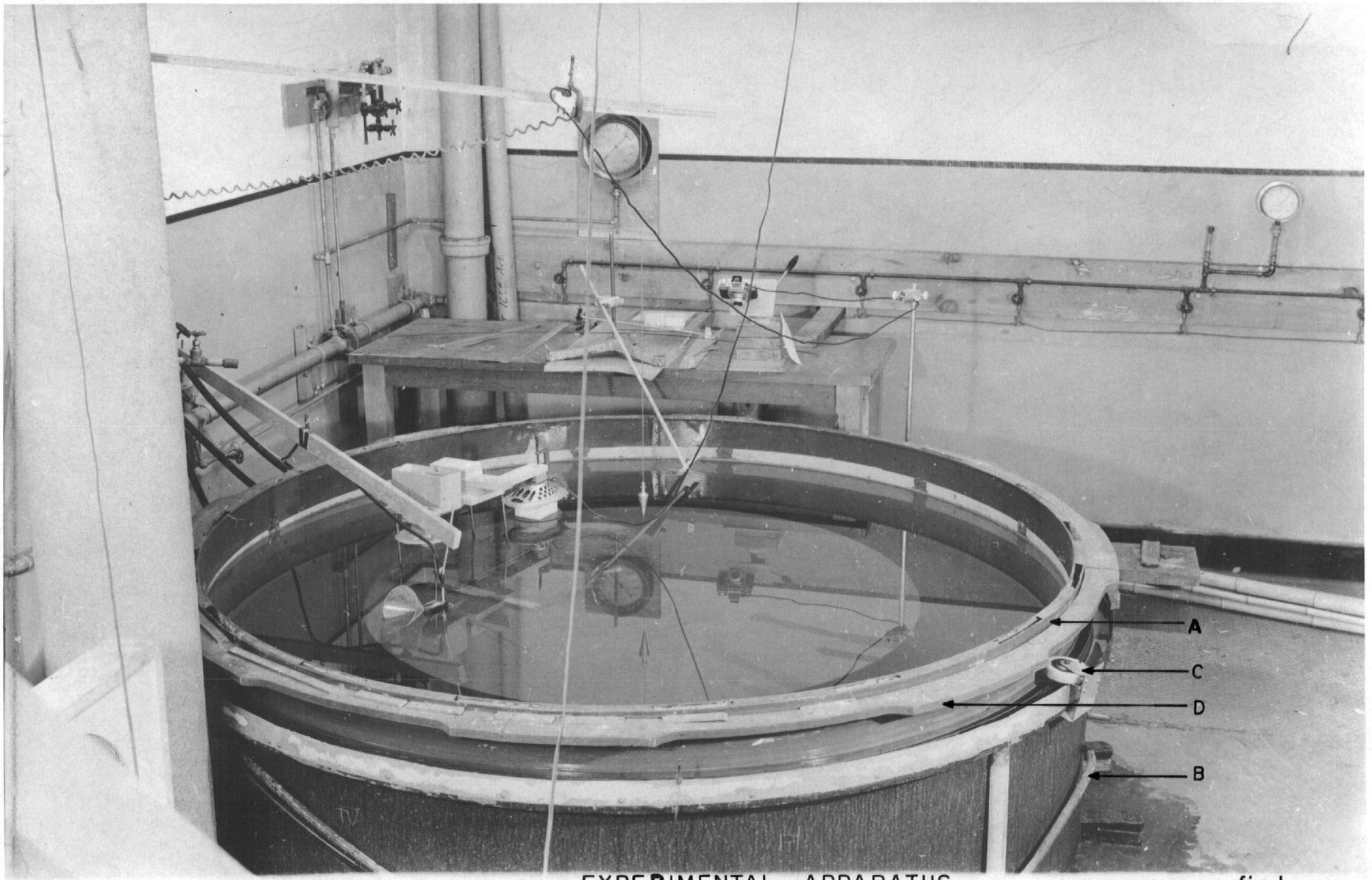

EXPERIMENTAL APPARATUS

fig.1

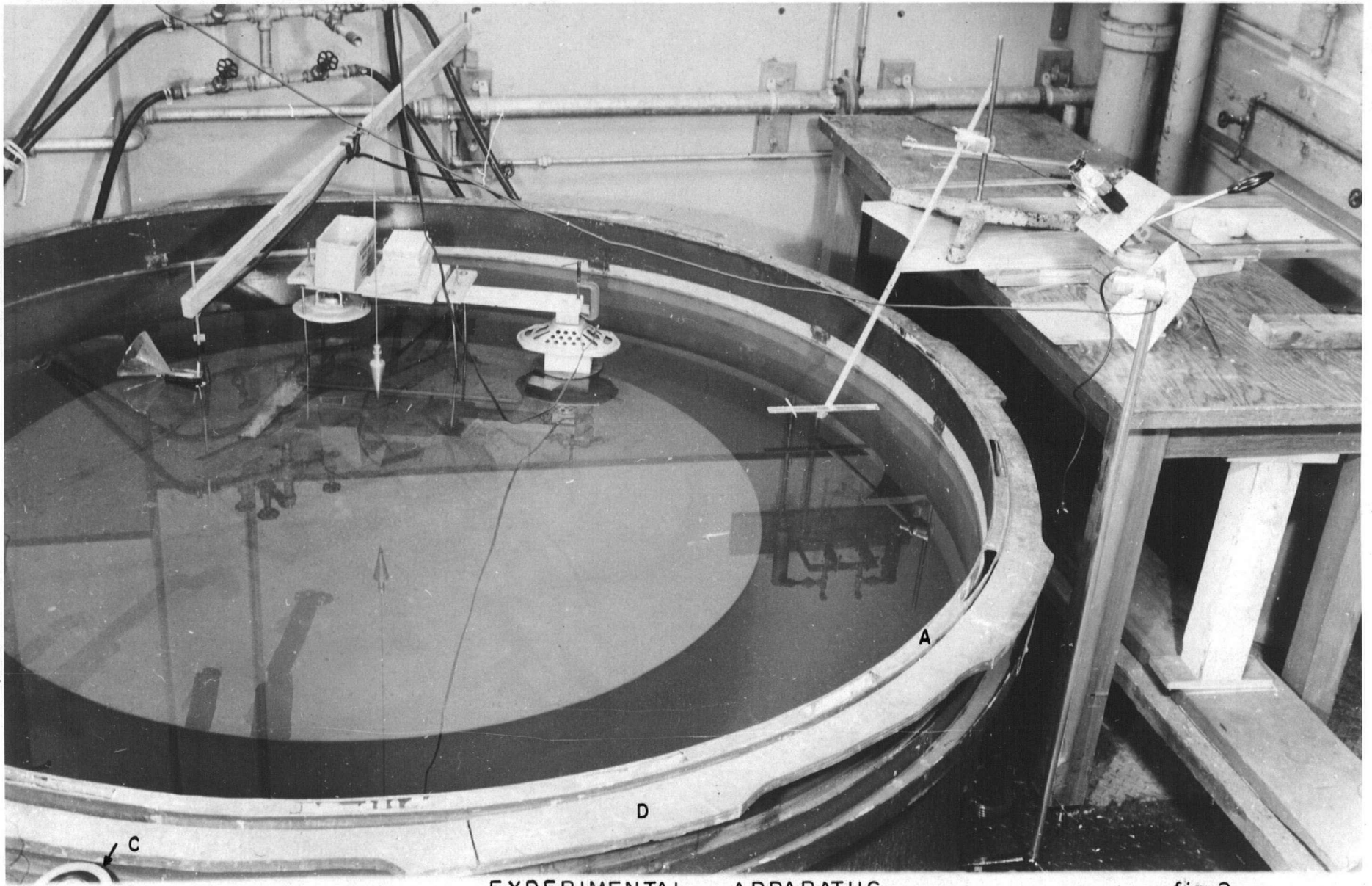

EXPERIMENTAL APPARATUS

fig.2

EXPERIMENTAL APPARATUS

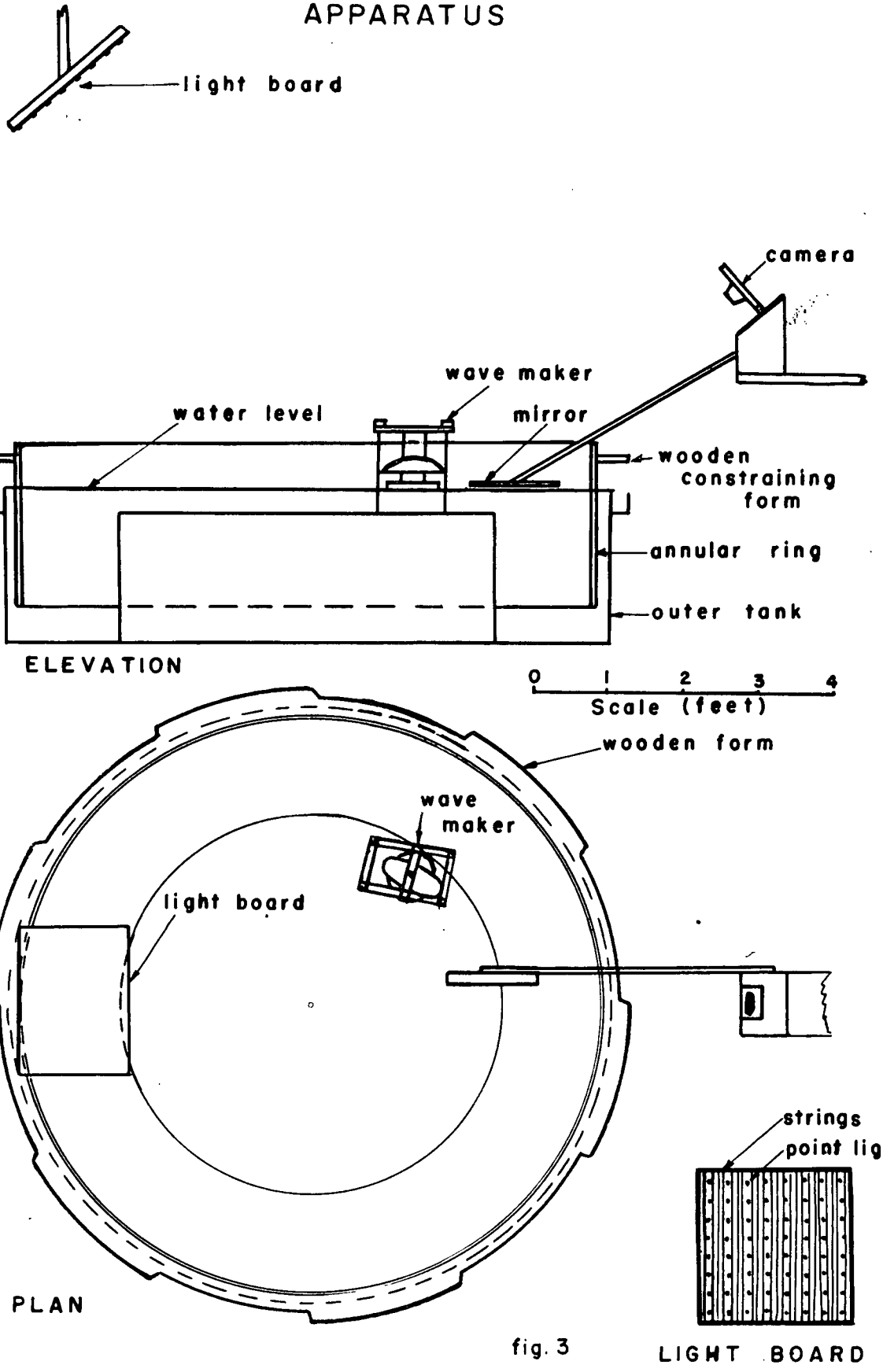

fig. 3

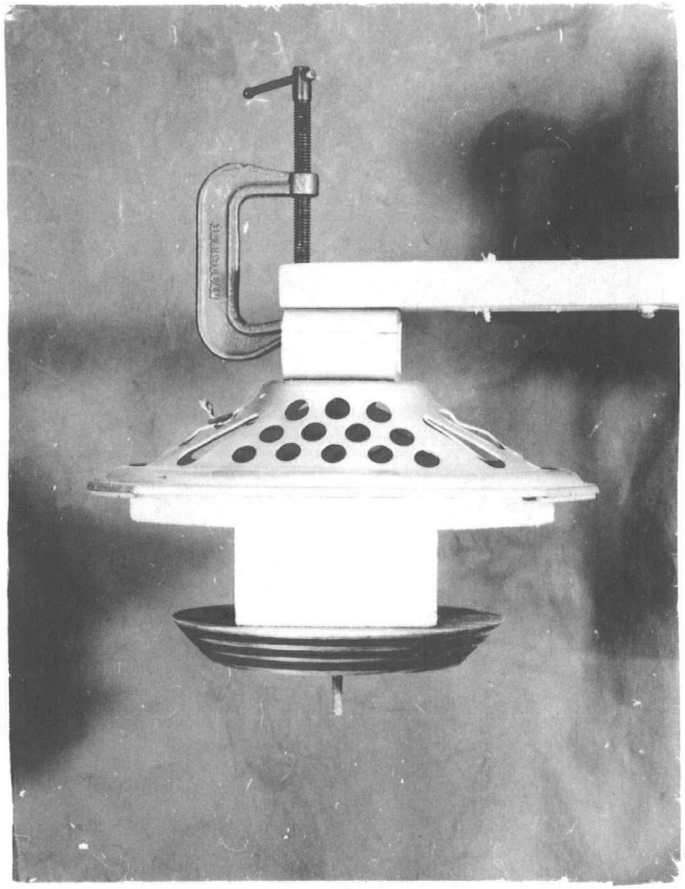

WAVEMAKER

fig. 4

WAVE PRODUCTION CIRCUIT

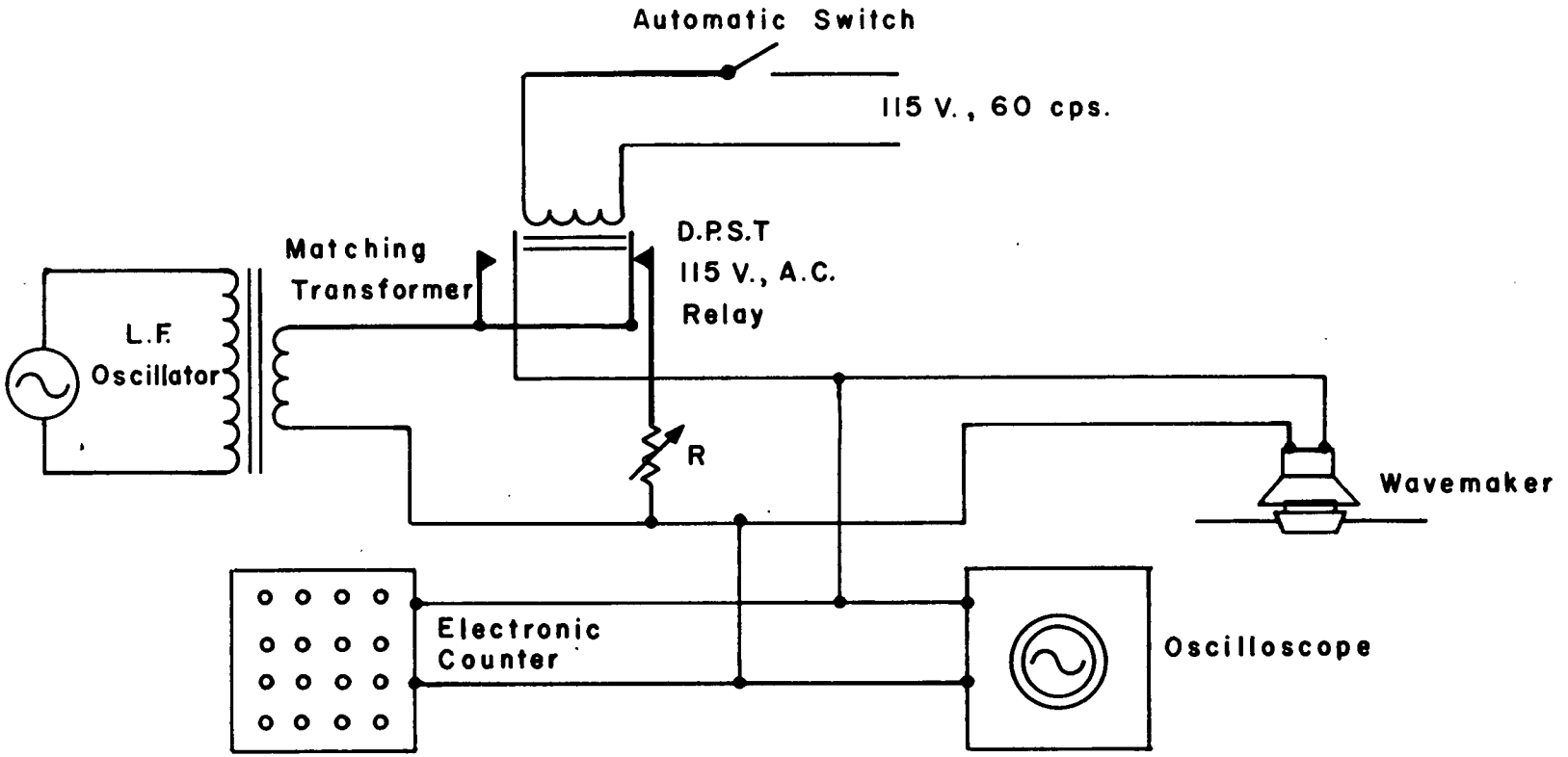

R = 10 ohm Potentiometer

fig. 5

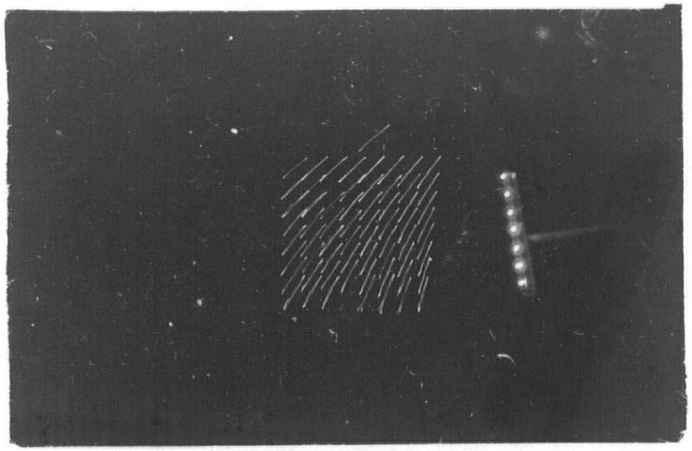

Amplitude With Flow. Accepted

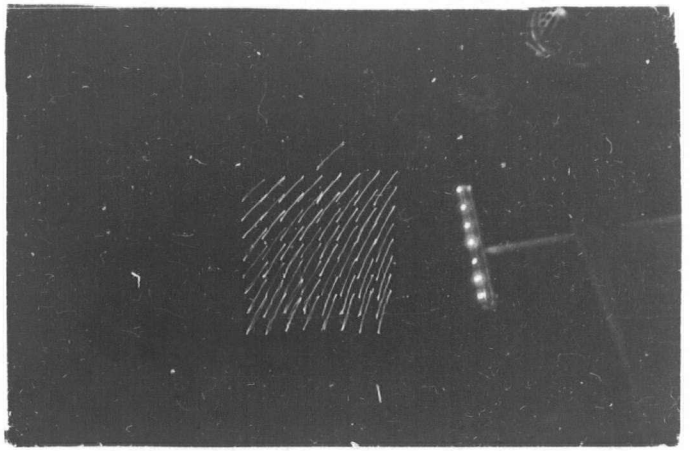

Amplitude With Flow. Accepted

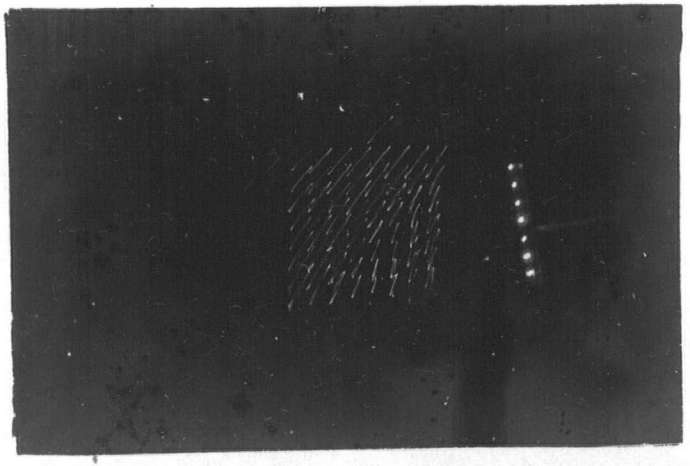

Amplitude With Flow. Rejected

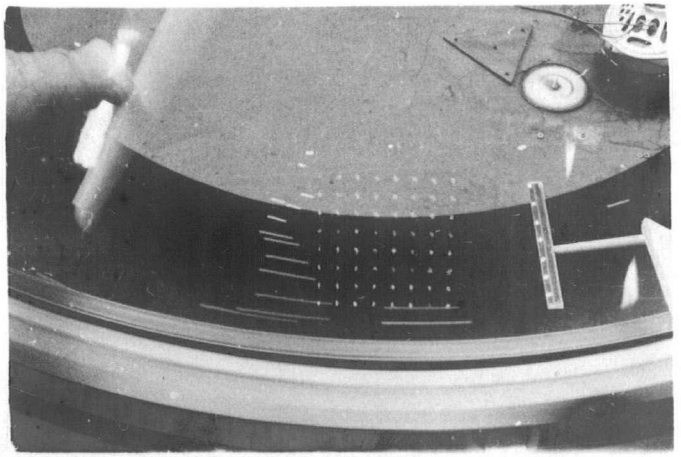

Current

AMPLITUDE AND CURRENT

fig. 6

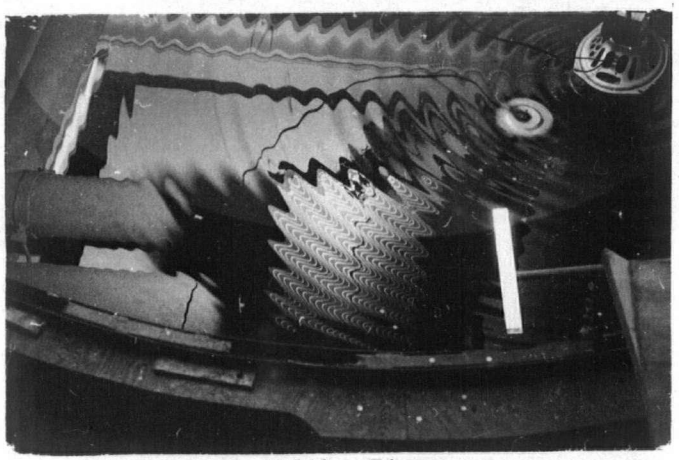

With Flow
(6 cps.)

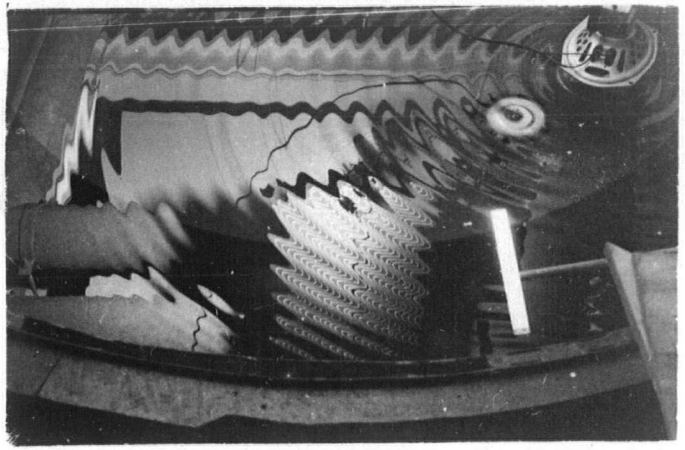

With Flow
(6 cps.)

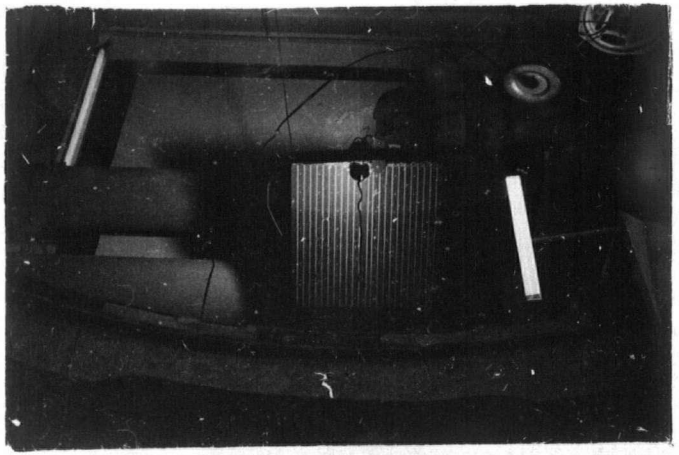

No Waves

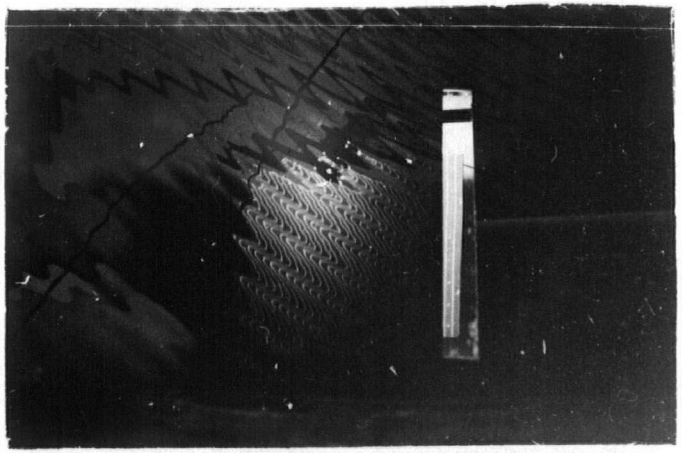

Without Flow
(10.5 cps.)

PHASE PHOTOGRAPHS

fig. 7

ENERGY PROPAGATION GEOMETRY

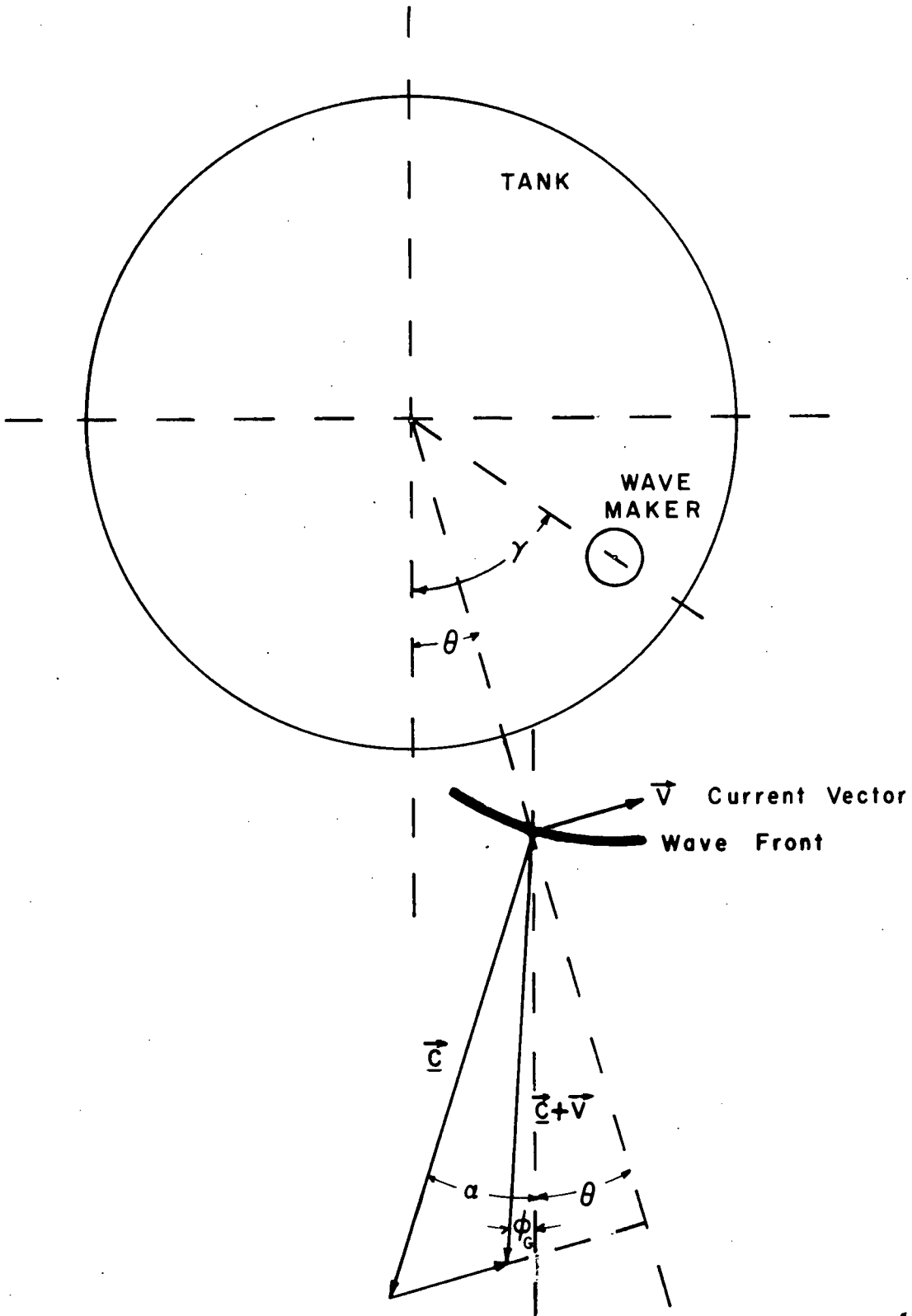

fig. 8

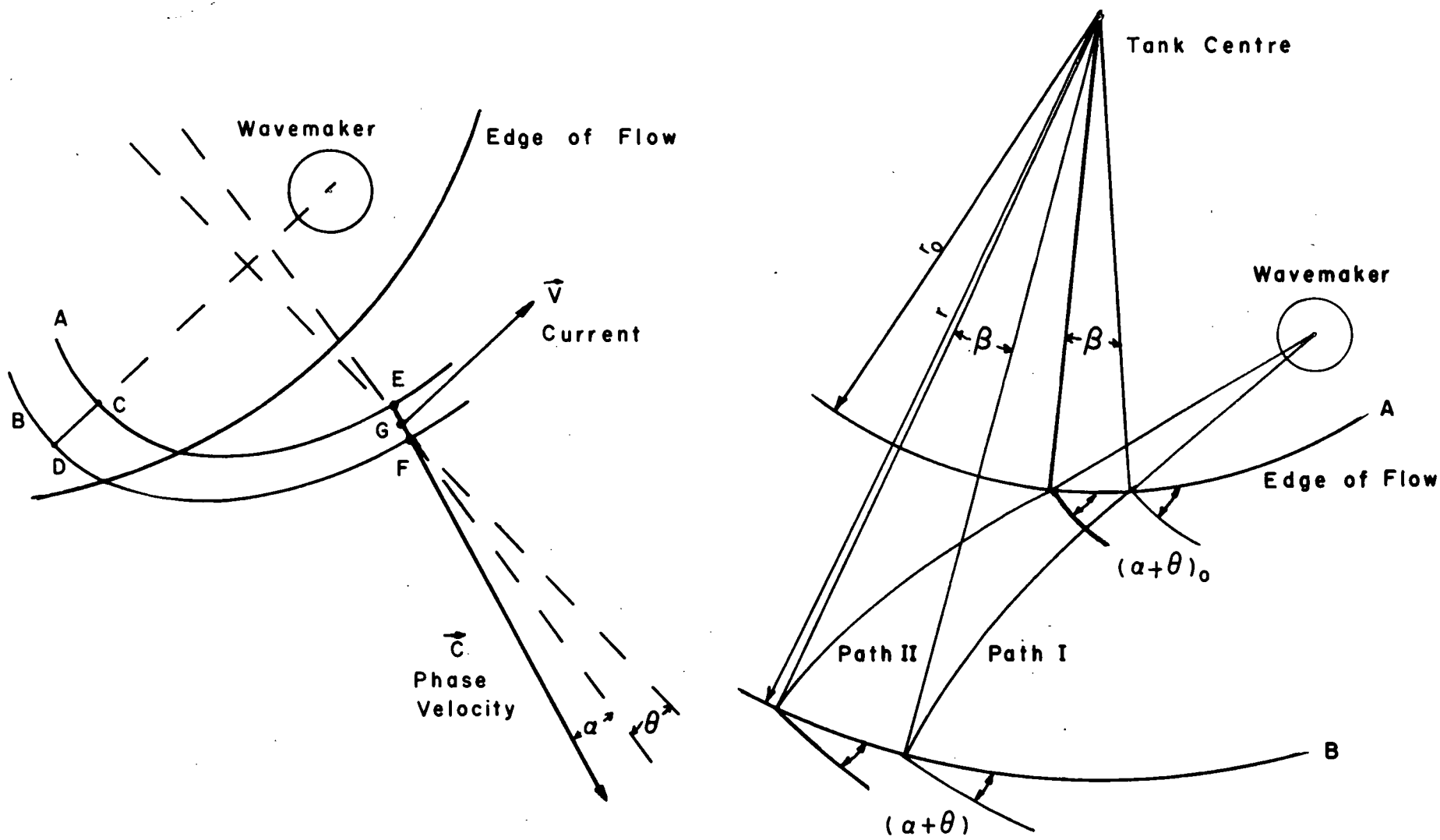
Wavemaker
Edge of Flow
$\vec{V}$
Current
A
B
C
D
E
G
F
$\vec{C}$
Phase
Velocity
α
θ
I. KINEMATIC FREQUENCY CONDITION
Tank Centre
r
r
β
β
Wavemaker
A
Edge of Flow
$(\alpha+\theta)_0$
Path II
Path I
B
$(\alpha+\theta)$
II. ZERO'TH ORDER KINEMATIC APPROXIMATION

fig. 9

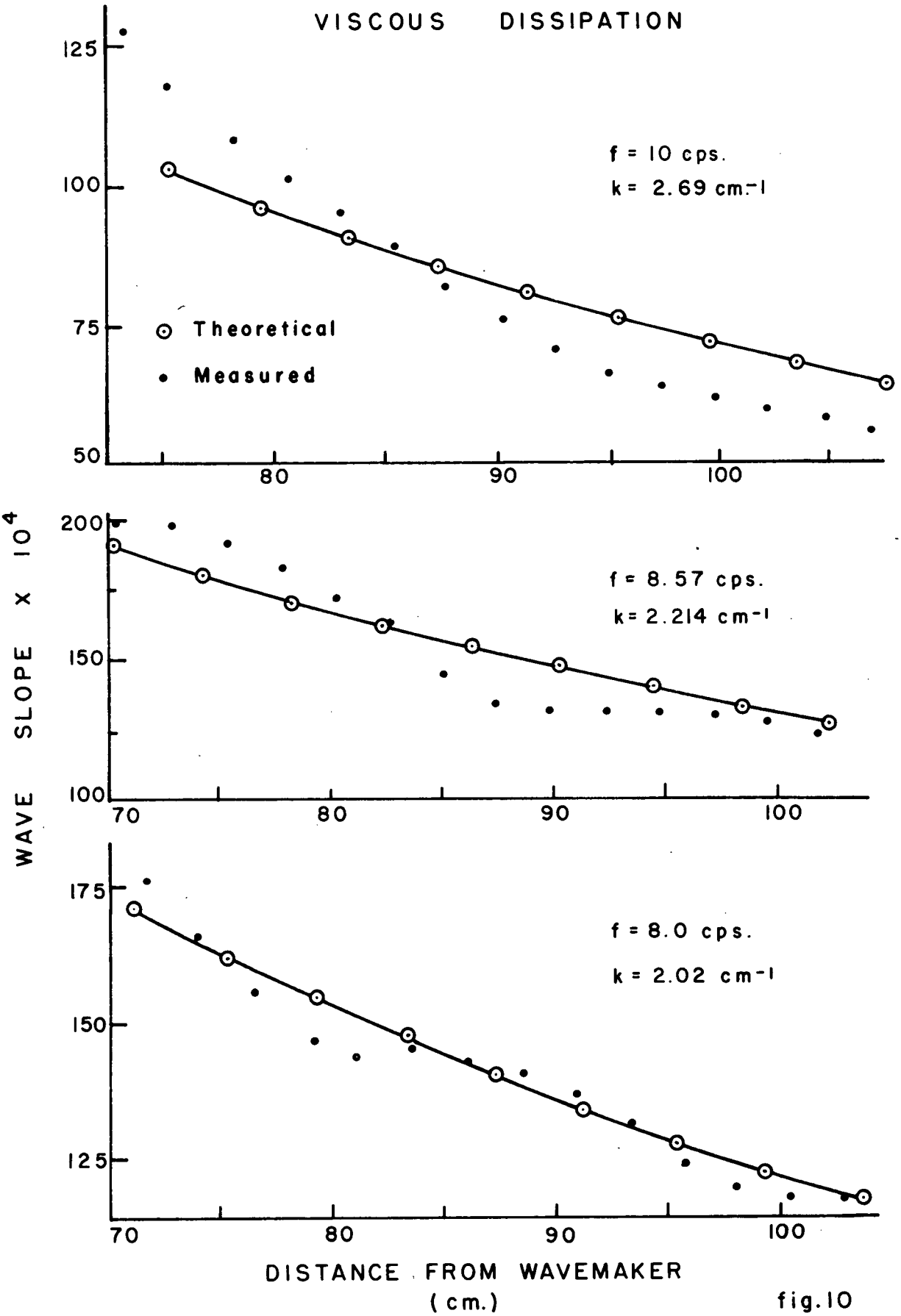
VISCOUS DISSIPATION
f = 10 cps.
k = 2.69 cm⁻¹
Theoretical
Measured
f = 8.57 cps.
k = 2.214 cm⁻¹
f = 8.0 cps.
k = 2.02 cm⁻¹
WAVE SLOPE X 10⁴
DISTANCE FROM WAVEMAKER
(cm.)

fig.10

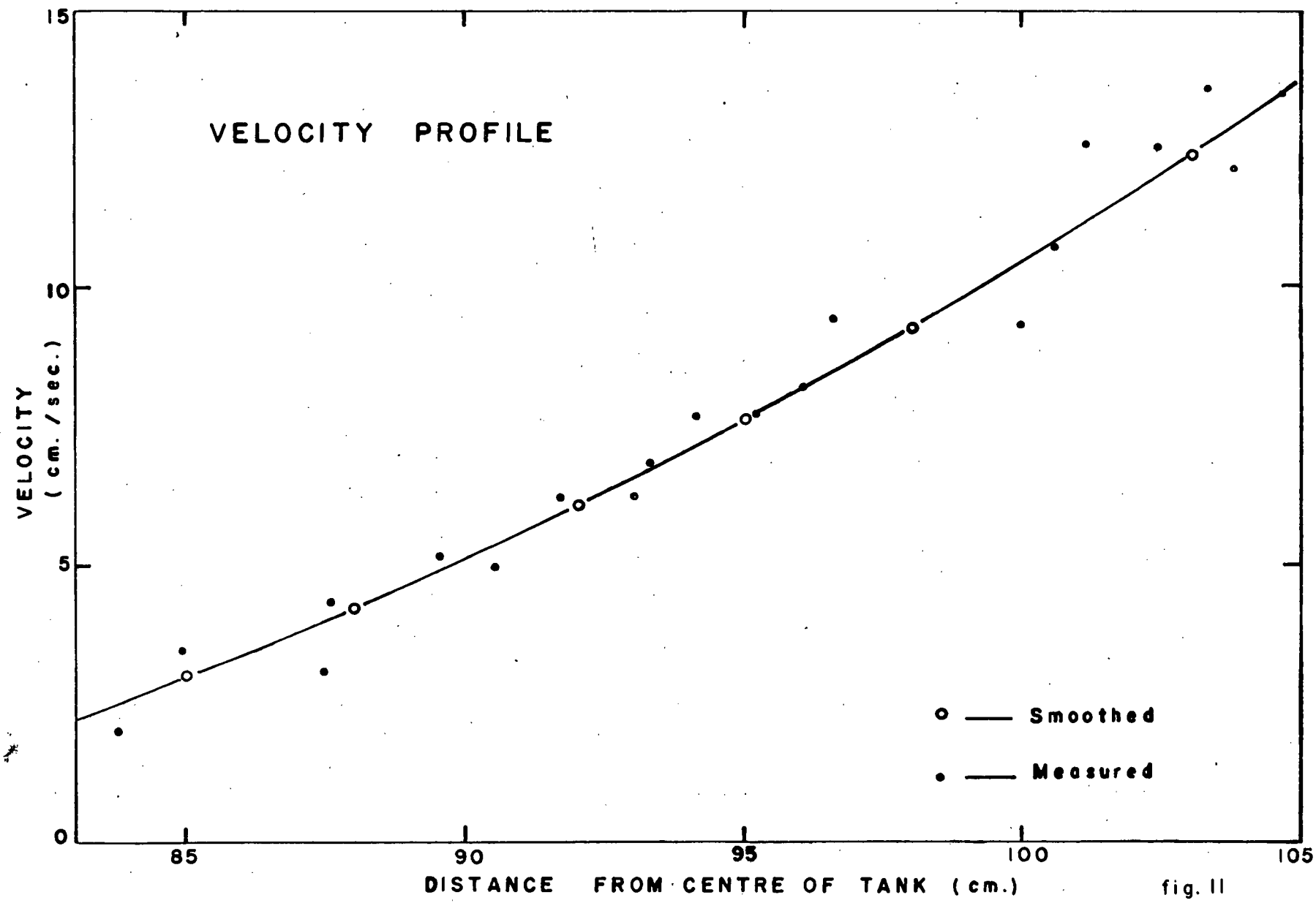
VELOCITY PROFILE
VELOCITY (cm. / sec.)
15
10
5
0
85
90
95
100
105
DISTANCE FROM CENTRE OF TANK (cm.)
Smoothed
Measured

fig. 11

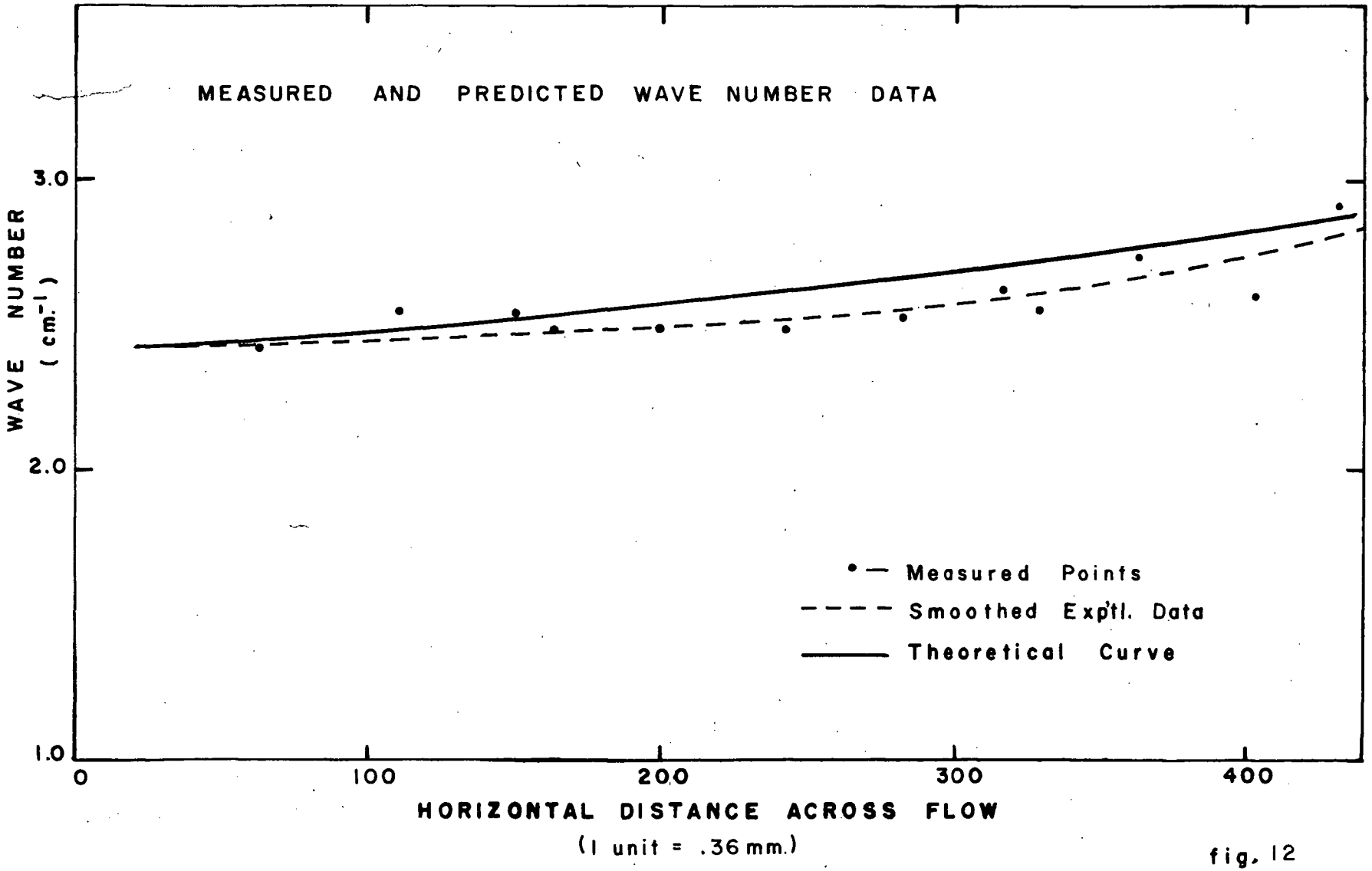
MEASURED AND PREDICTED WAVE NUMBER DATA
WAVE NUMBER (cm.⁻¹)
3.0
2.0
1.0
0
100
200
300
400
HORIZONTAL DISTANCE ACROSS FLOW
(1 unit = .36 mm.)
Measured Points
Smoothed Expt'l. Data
Theoretical Curve

fig. 12

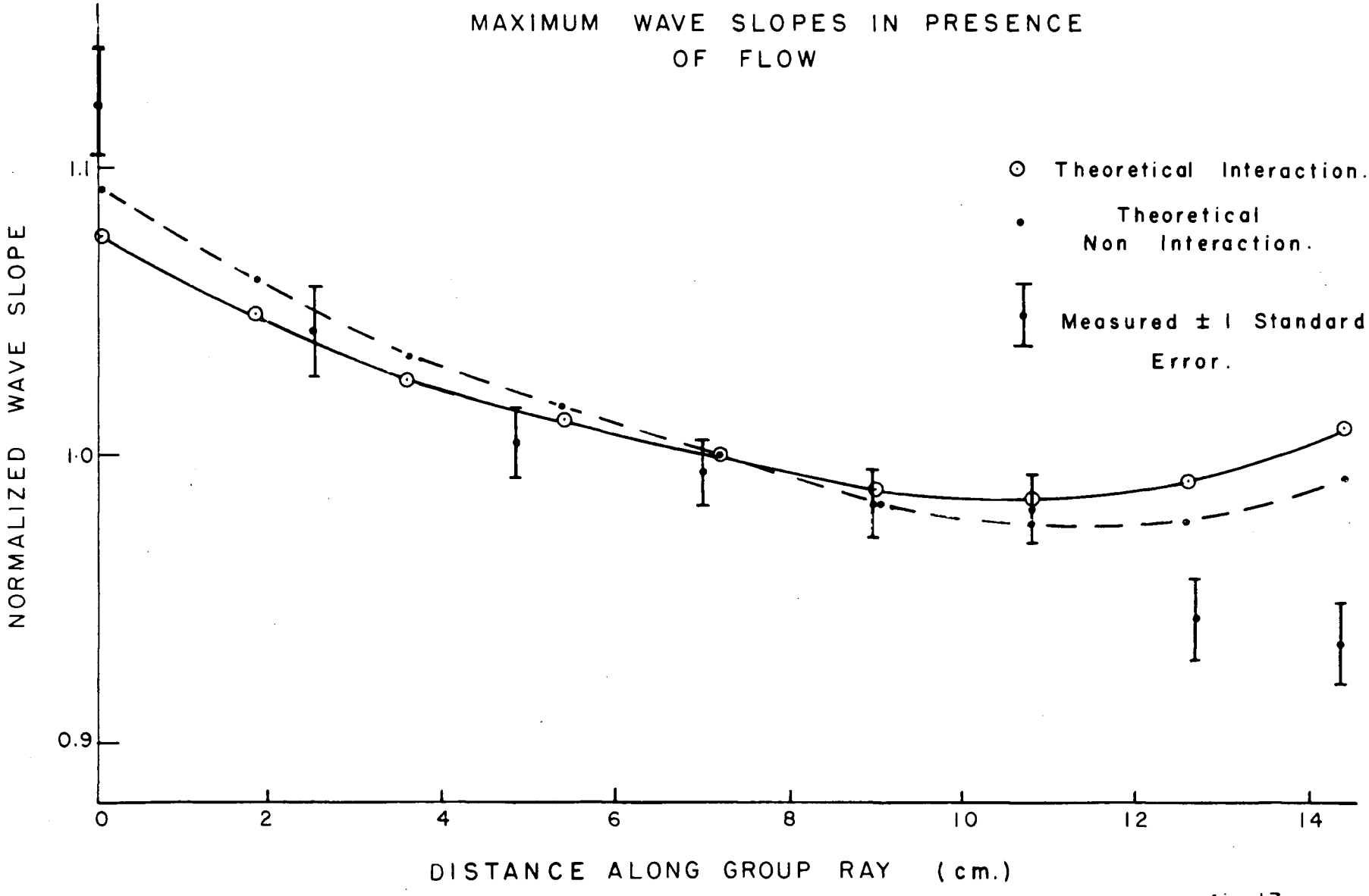
MAXIMUM WAVE SLOPES IN PRESENCE OF FLOW
NORMALIZED WAVE SLOPE
1.1
1.0
0.9
0
2
4
6
8
10
12
14
DISTANCE ALONG GROUP RAY (cm.)
Theoretical Interaction.
Theoretical Non Interaction.
Measured ± 1 Standard Error.

fig. 13

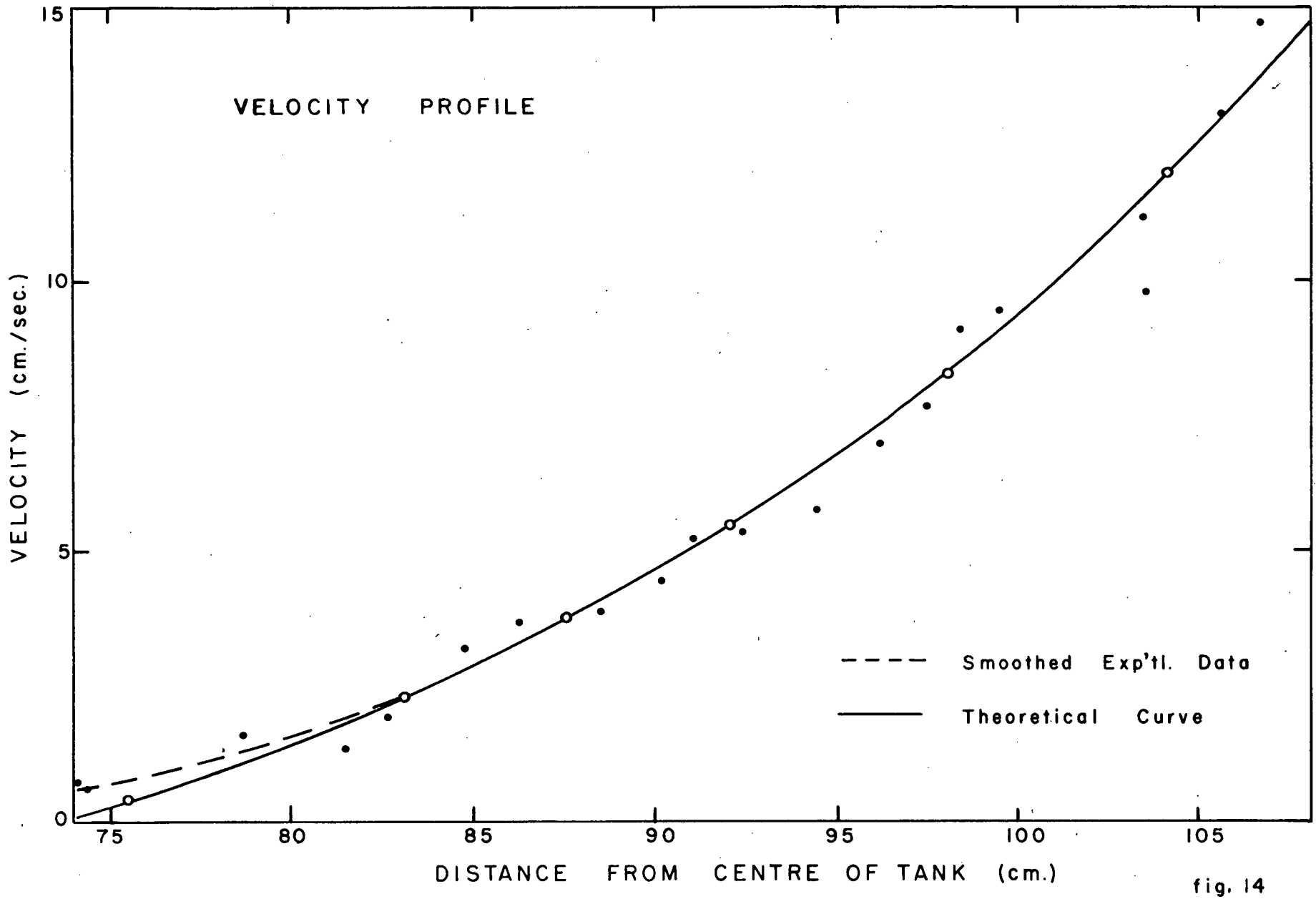
VELOCITY PROFILE
VELOCITY (cm./sec.)
15
10
5
0
75
80
85
90
95
100
105
DISTANCE FROM CENTRE OF TANK (cm.)
Smoothed Exp'tl. Data
Theoretical Curve

fig. 14

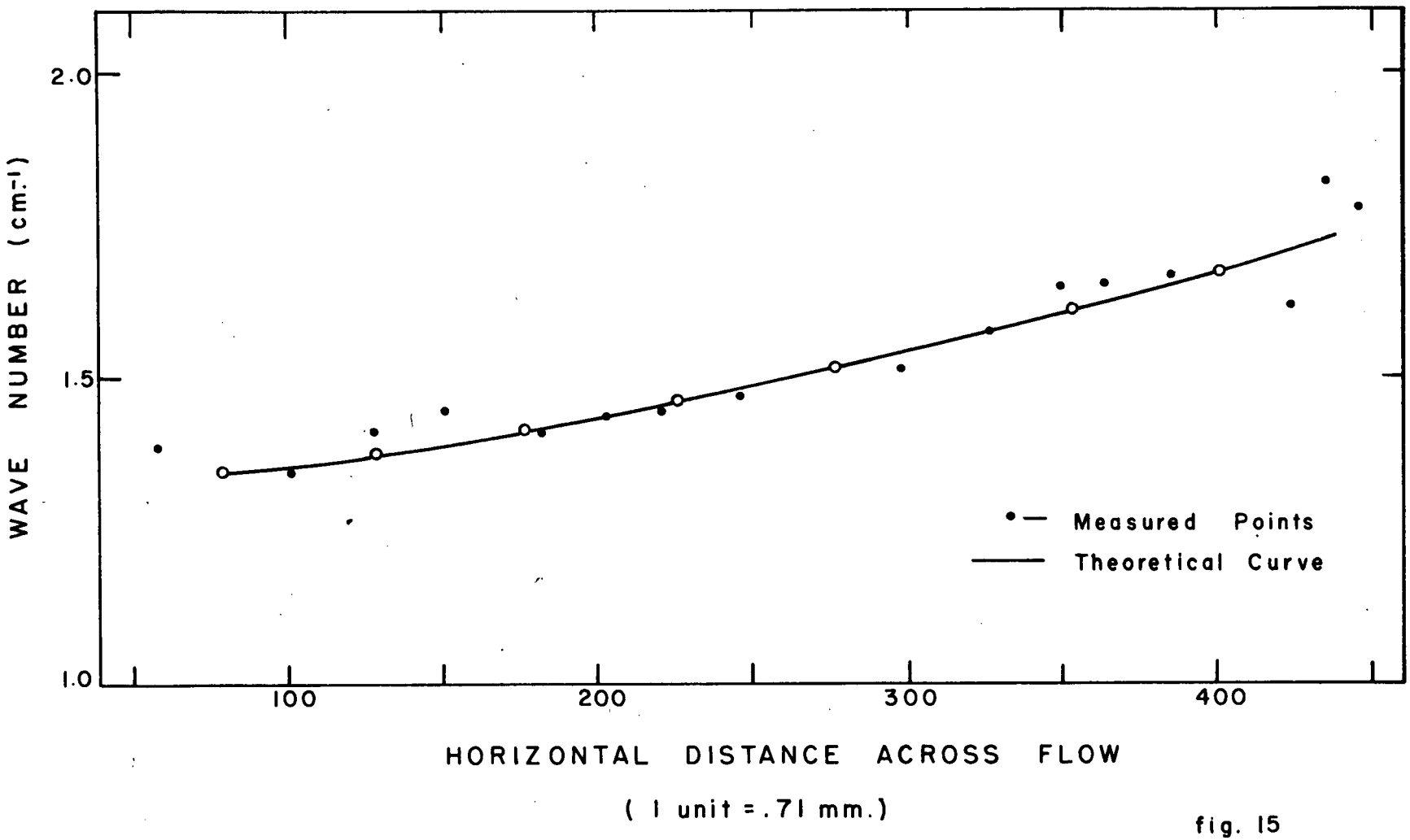
WAVE NUMBER (cm.⁻¹)
2.0
1.5
1.0
100
200
300
400
Measured Points
Theoretical Curve
HORIZONTAL DISTANCE ACROSS FLOW
(1 unit = .71 mm.)

fig. 15

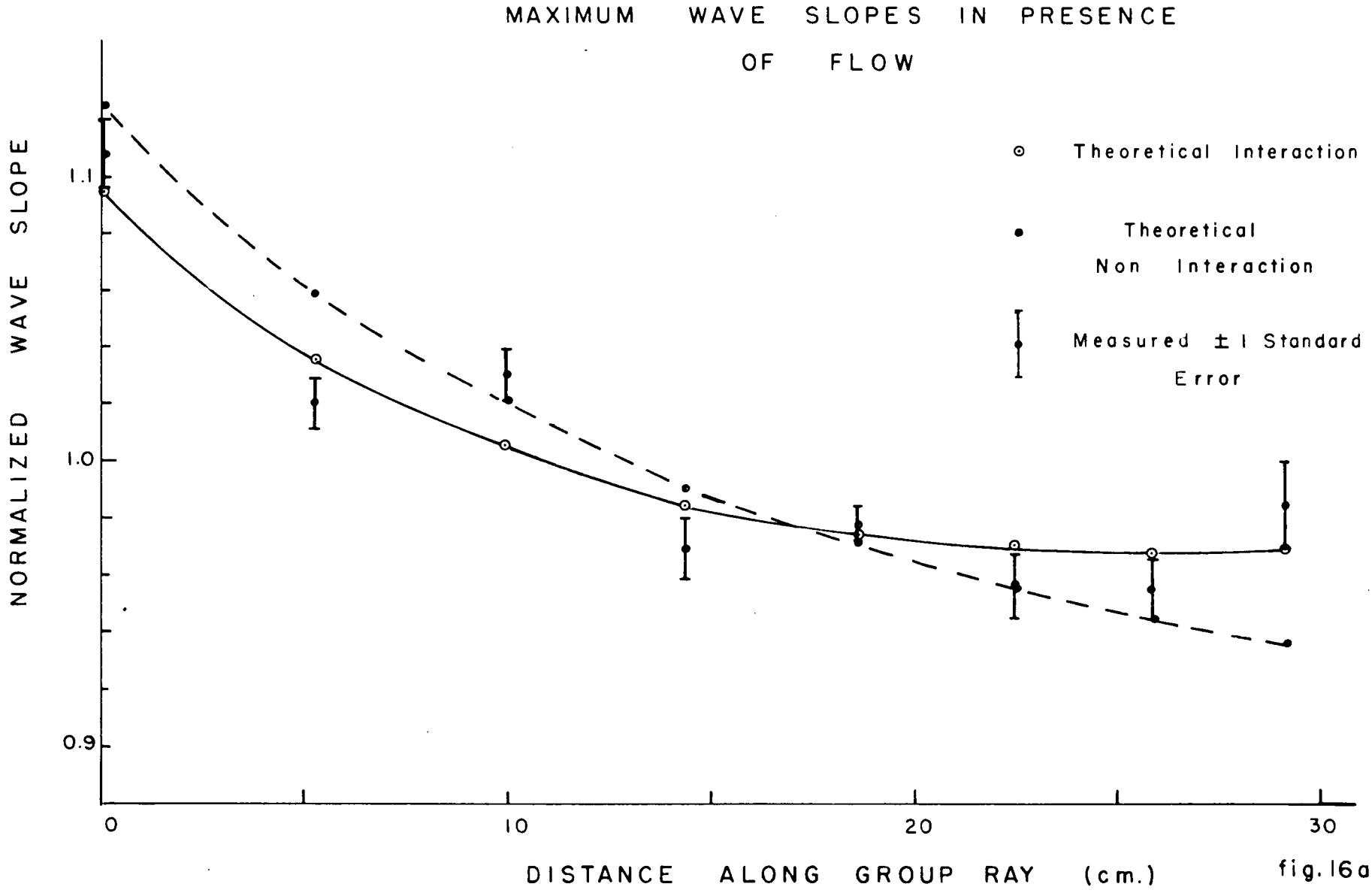
MAXIMUM WAVE SLOPES IN PRESENCE OF FLOW
NORMALIZED WAVE SLOPE
1.1
1.0
0.9
0
10
20
30
DISTANCE ALONG GROUP RAY (cm.)
Theoretical Interaction
Theoretical Non Interaction
Measured ± 1 Standard Error

fig. 16a

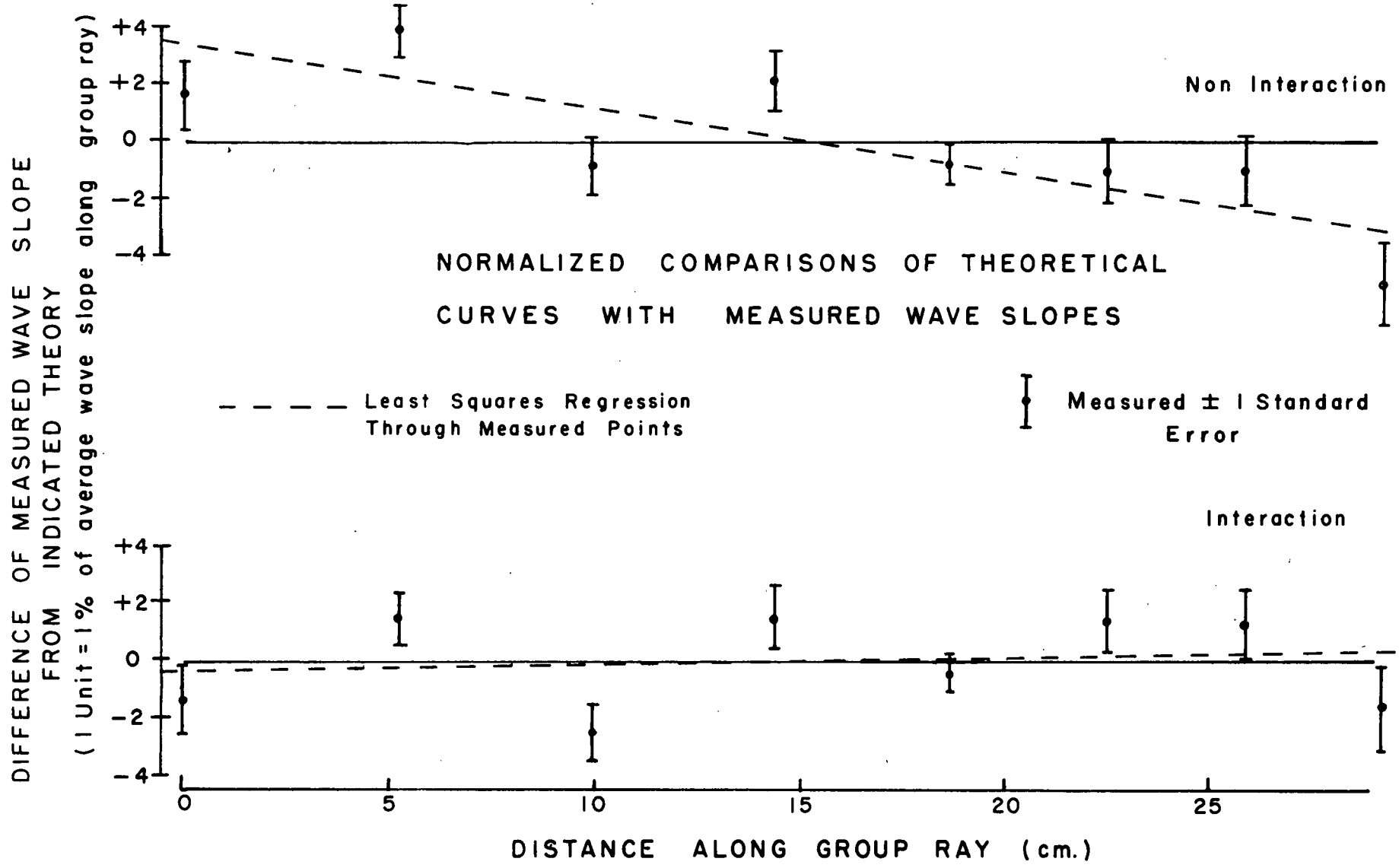
Non Interaction
NORMALIZED COMPARISONS OF THEORETICAL
CURVES WITH MEASURED WAVE SLOPES
Least Squares Regression
Through Measured Points
Measured ± 1 Standard
Error
Interaction
DIFFERENCE OF MEASURED WAVE SLOPE
FROM INDICATED THEORY
(1 Unit = 1% of average wave slope along group ray)
+4
+2
0
−2
−4
0
5
10
15
20
25
DISTANCE ALONG GROUP RAY (cm.)

fig. 16 b

LINES OF CONSTANT PHASE

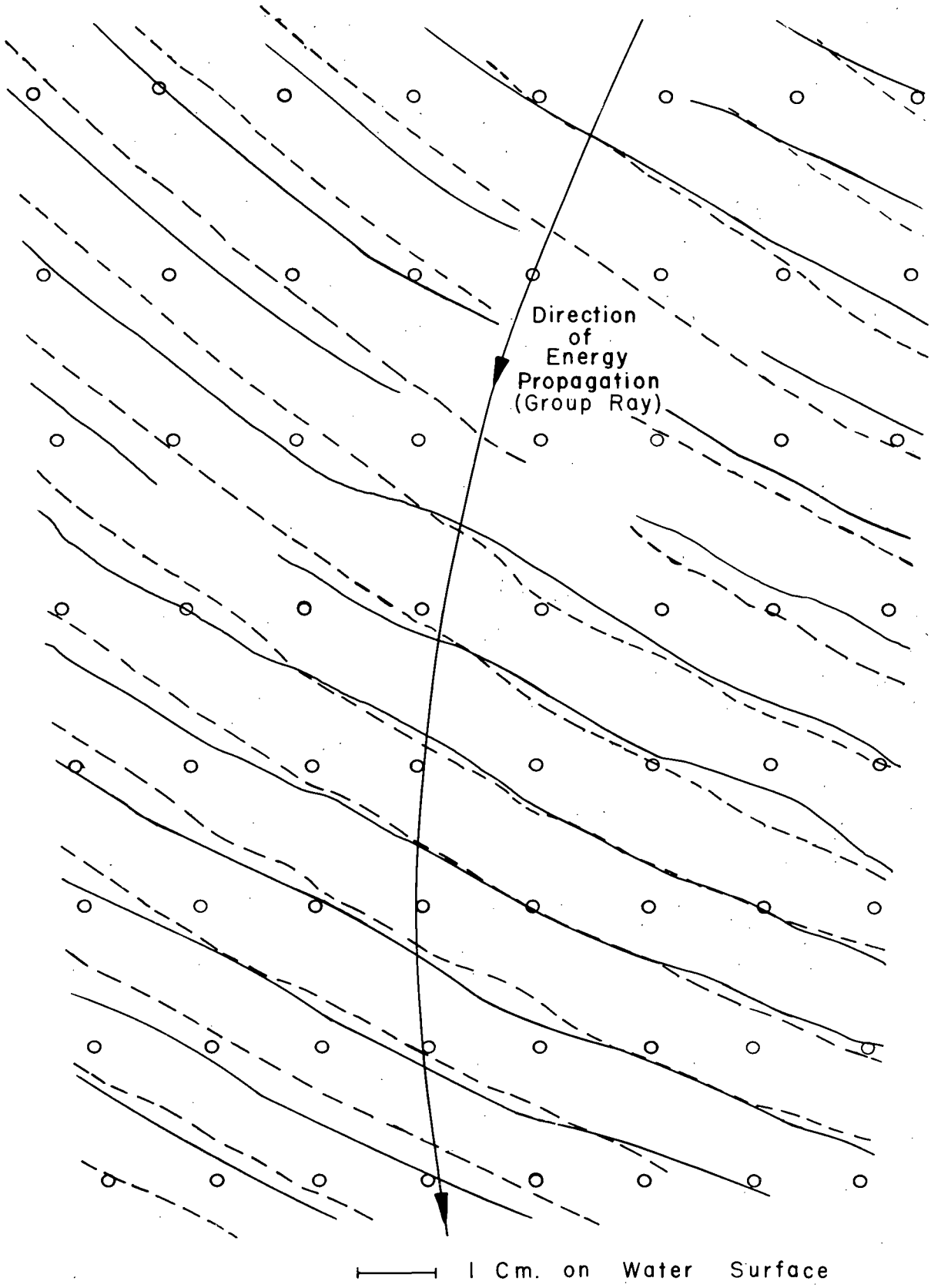

fig. 17

LINES OF CONSTANT PHASE

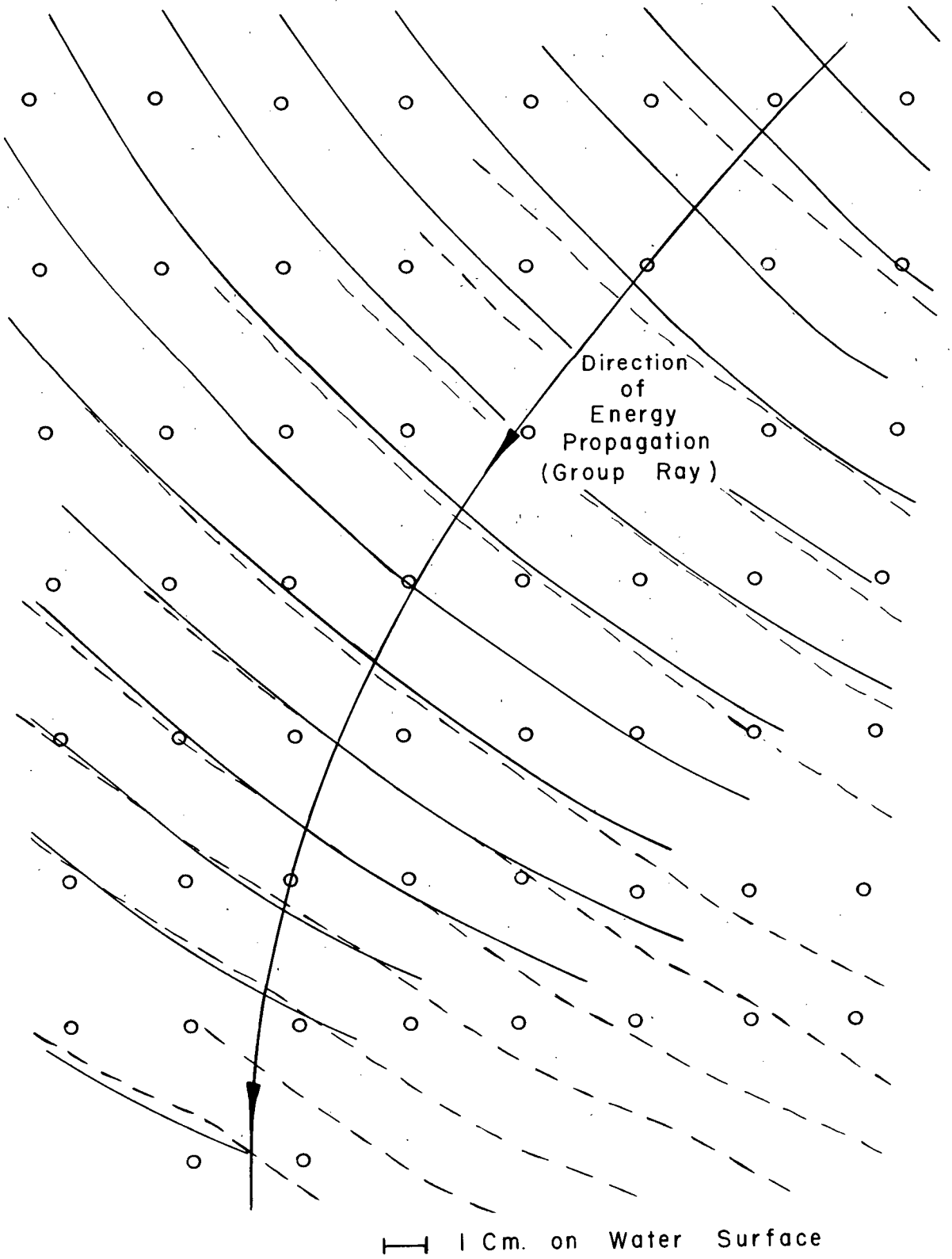

fig. 18

LINES OF CONSTANT PHASE

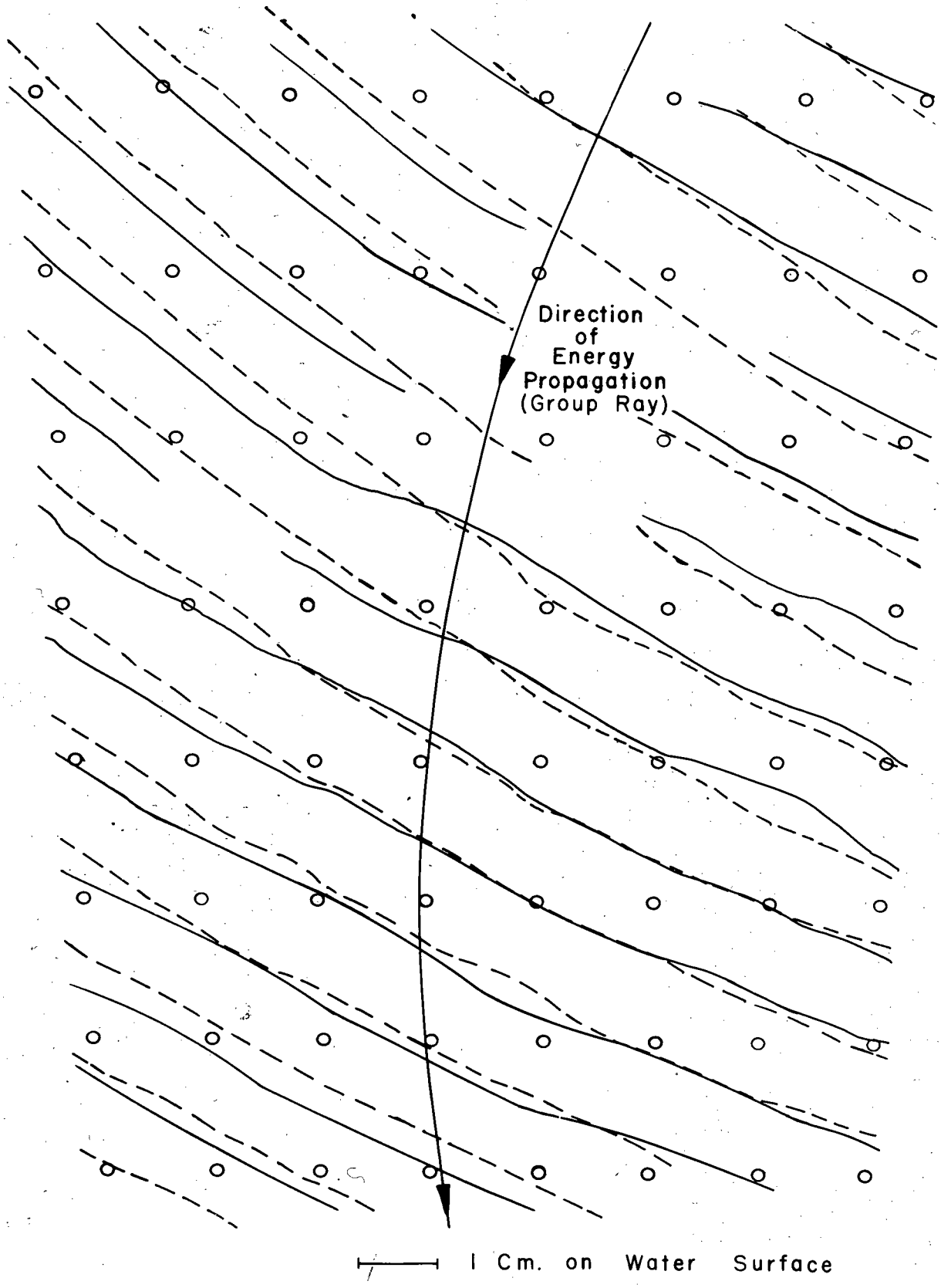

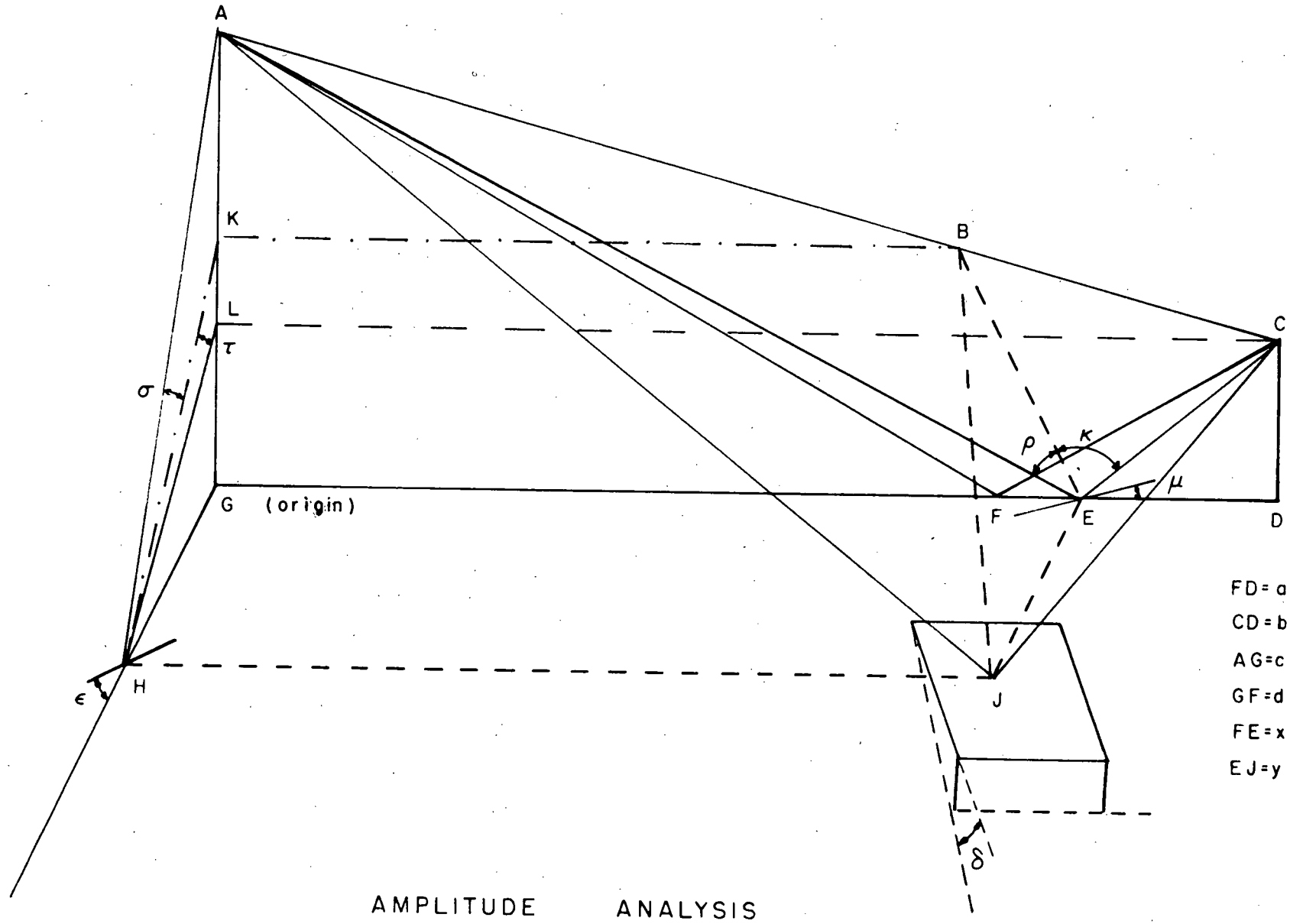

AMPLITUDE ANALYSIS

fig. 19